RESONANT CONVERTER DESIGN
FOR
PORTABLE POWER APPLICATION

By

Nur Afidatul Anis Bt Azmi

Dissertation submitted in partial fulfillment
of the requirements for the
Bachelor of Engineering (Hons)
(Electrical and Electronics Engineering)

SEPTEMBER 2011

Universiti Teknologi PETRONAS
Bandar Sri Iskandar
31750 Tronoh
Perak Darul Ridzuan

CERTIFICATION OF APPROVAL

RESONANT CONVERTER DESIGN FOR PORTABLE POWER APPLICATION

By

Nur Afidatul Anis Bt Azmi

A project dissertation submitted to the

Electrical and Electronics Engineering Programme

Universiti Teknologi PETRONAS

in partial fulfillment of the requirement for the

BACHELOR OF ENGINEERING (Hons)

(ELECTRICAL AND ELECTRONICS ENGINEERING)

Approved by:

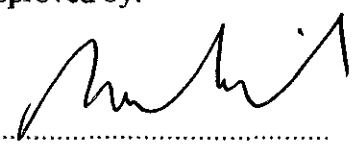

.....

(Dr Nordin Bin Saad)

Project Supervisor

Nordin Saad
:turer
ctrical & Electronics Engineering Programme
iversiti Teknologi PETRONAS
'50 Tronoh,
ak Darul Ridzuan, MALAYSIA

UNIVERSITI TEKNOLOGI PETRONAS

TRONOH, PERAK

SEPTEMBER 2011

CERTIFICATION OF ORIGINALITY

This is to certify that I am responsible for the work submitted in this project, that the original work is my own except as specified in the references and acknowledgement, and that the original work contained herein have not been undertaken or done by unspecified sources or persons.

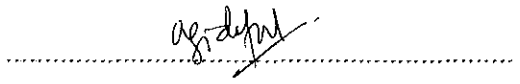

(NUR AFIDATUL ANIS BT AZMI)

ACKNOWLEDGEMENT

First of all, I would like to express my gratitude and praise to God for His guidance and blessings upon completion of the Final Year Project 2011. Special thanks to my supervisor, Dr Nordin Bin Saad and my co-supervisor Mr. Saiful Azrin for their guidance and advices throughout this project.

I would like to extend a special thank you to my family and friends for moral supports and motivations in helping me all the way through until the end. Thank you to all Universiti Teknologi PETRONAS lecturers, technicians and everyone involved, directly or indirectly for helping me upon my completion of the Final Year Project. God bless you.

ABSTRACT

The well established advantages of resonant converters have led to their increasing attraction. Resonant converters topologies can be used to increase circuit switching speeds, allowing the cost of circuit magnetic to be reduced, while still keeping switching losses to a minimum. Full wave rather than half wave topologies are generally used, as they generate less EMI. With the advantages, resonant converters can be used in portable power application. This project will go for details of resonant converters behavior, characteristic, type and mode of operation to design the suitable resonant converter circuit which meet the requirement of related portable power application. This project will go through modeling, simulation and analysis approach.

TABLE OF CONTENTS

LIST OF FIGURES

LIST OF TABLES

CHAPTER 1

INTRODUCTION

1.1 Background of study

The number of electronics application that have become portable in the last 20 years has risen dramatically with the evolution of battery technologies. Along with battery technology enhancements, a lots of supports for electronic components and technologies have blossomed, which have further fueled the transition to portable power. The rapid progression to smaller, more powerful microprocessors and less expensive electronic components have facilitated miniaturization of mobile applications.

Portable power application has used in a wide range of areas, including biomedical, uninterruptible power supply (UPS), future renewable energy system and many more. Take biomedical field as an example, the implantable biomedical devices are used as pacemakers, monitoring devices, artificial hearts and left ventricular assist devices (LVAD). Supplying power to those devices for long term operation is a challenging task. Traditionally, implantable batteries are used. However, the batteries have limited energy storage and life-span [13].

People have paid attention to the resonant power converters which offer many advantages over the PWM power converters, such as low switching losses at higher switching frequencies, easier EMI filtering, reduced component stress and higher efficiency [2]. The chief advantage of resonant converters is reduced switching losses [1].

There are many topologies of resonant converters such as series resonant converter (SRC), parallel resonant converter (PRC), ZCS- Push Pull resonant converter, LLC resonant converter and many more. The PRC is preferable for

voltage regulator applications having wide load variation, such as switching power supplies, mainly because of the load independent feature [2].

1.2 Problem statement

Many applications requires power electronic converter that provides: high efficiency, small switching losses, snubberless, and low electromagnetic interference (EMI) problem. In applications that requires high power, the converter needs to be operated at high switchings (increased frequency). However, increasing the frequency of operation will increase switching losses and hence reduces system efficiency. Due to this concern, this work will look into the design of a suitable converter that can meet these requirements.

1.3 Objectives

The objectives of this project are:

- To determine the appropriate component size for resonant converter (L,C) for a certain requirement.
- To obtain low losses converter.
- To identify the combination of converter topologies or switching strategies that in zero voltage switching and/or zero current switching for the circuit.
- To design the resonant converter

1.4 Scope of study

The scope of this project consists of research, modelling & simulation and analysis. The research is important for better understanding on the theory and concept of resonant converter. Modelling & simulation using Pspice tools is to test or manipulate the value/measurement that produced from the research. Lastly analysis part is to analyze whether the outcomes of the simulation meet the requirement or not. Then the project will proceed with the documentation of the resonant converter for portable power application.

CHAPTER 2

LITERATURE REVIEW

2.1 Operation of Resonant Converters

Resonant converters consist of many topologies. The difference between each topology is it resonant tank network.

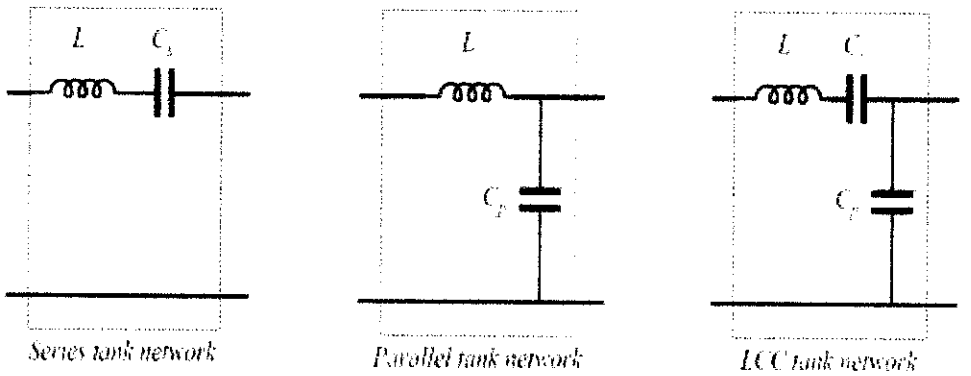

Figure 1: Types of resonant tank network

2.1.1 Series Resonant Converter (SRC)

In series resonant converter, the load is connected to the resonant circuit in series and the output voltage is obtained from the resonant current. The main characteristics of the SRC include [2]:

- Inherent overload protection
- Load sensitivity
- Poor operation at no load

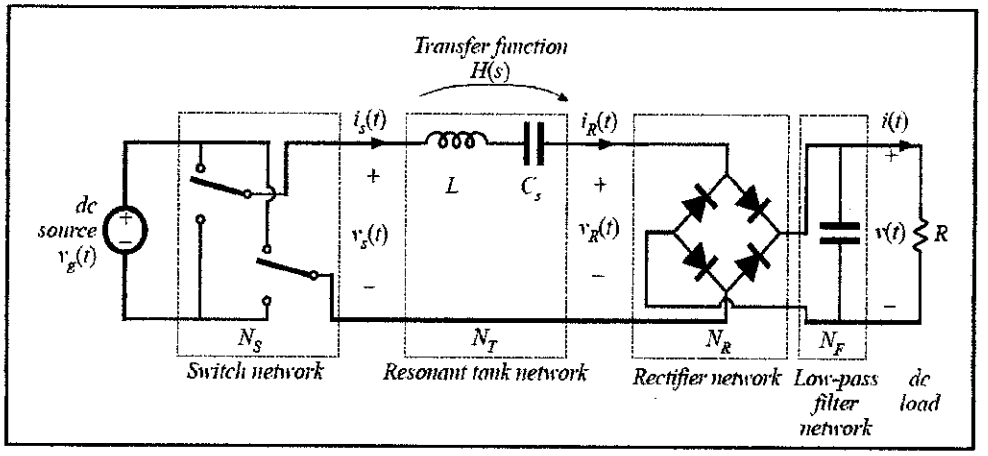

Figure 2: Series resonant dc-dc converter

Resonant frequency (f_r) exists in the resonant converter whose voltage and current waveforms vary sinusoidal during one or more subintervals of each switching period [14]. Resonance happens when the inductive reactance (X_L) and capacitive reactance (X_C) are equal in absolute values and the two impedances cancel each other out and the total impedance drops to zero.

$$\text{fs} = \text{switching frequency} = \frac{1}{T_s} \tag{1}$$

$$\text{fr} = \text{resonant frequency} = \frac{1}{2\pi\sqrt{L_r C_r}} \tag{2}$$

The ratio of the output dc voltage to the supply voltage is the gain of the converter [3].

V_{dc}=supply voltage

V_o=output voltage

$$\text{M=gain=} \frac{V_o}{V_{dc}} \tag{3}$$

The characteristic impedance of the tank is defines as [3]:

$$Z_c = \sqrt{\frac{L_r}{C_r}} \tag{4}$$

The load factor of the converter is defines as [3]:

$$Q = \frac{Z_c}{R_{load}} \tag{5}$$

2.1.2 Parallel Resonant Converter (PRC)

The parallel resonant converter in which the load is usually connected to the resonant capacitor in parallel, and the output voltage is obtained from the voltage across the resonant capacitor. The characteristic of PRC are [2]:

- Load insensitivity
- No load operation
- Need of overload protection

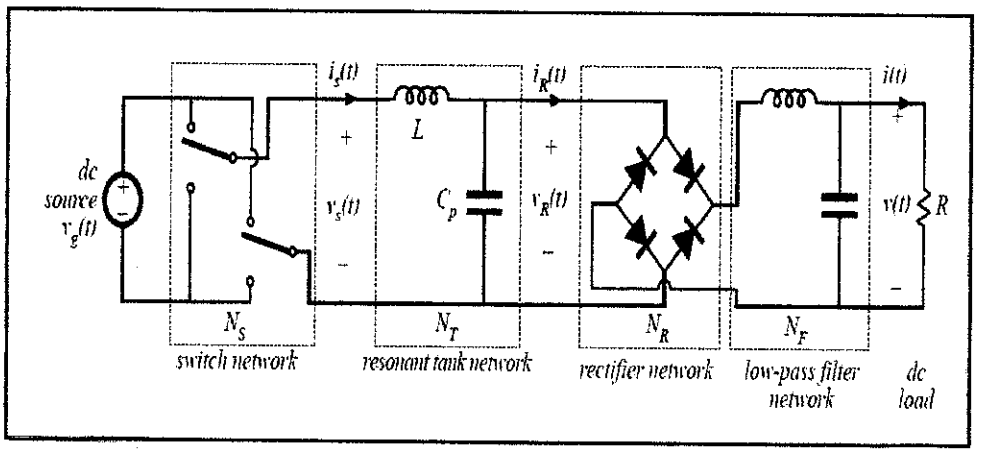

Figure 3: Parallel resonant dc-dc converter

2.2 Switching Losses

Switching losses are created as a result of a simultaneous exposure of MOSFET to high voltage and current during a transition between the open and closed states [6]. Ideally, there are two ways to realise near zero-switching loss. One is zero current switching(ZCS) and the other is zero voltage switching(ZVS) [4]. ZCS circuit shapes the current waveform, while ZVS circuit shapes the voltage waveform [5].

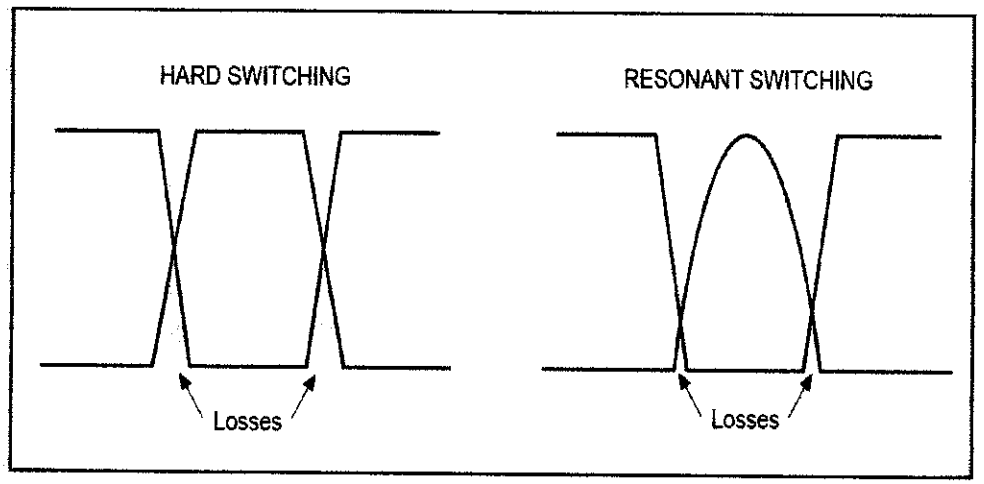

Figure 4: Current and voltage waveforms of hard and resonant switching systems

2.2.1 Zero Current Switch(ZCS)

Typical ZCS consists of a switch(S), in series with the resonant inductor(L_r), and the resonant capacitor(C_r) connected in parallel. Energy is supplied by a current source [5].

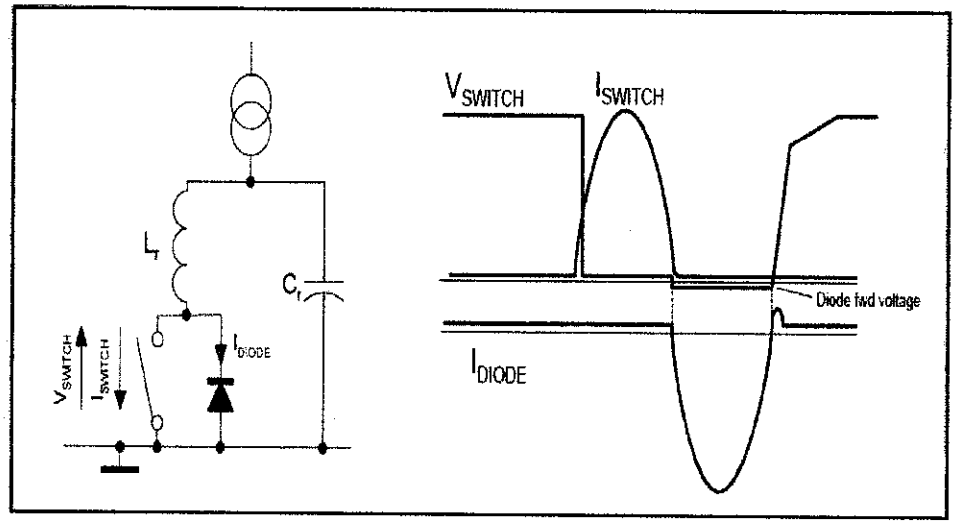

Figure 5: Full-wave zero-current switch - topology and waveform

When the switch S is off, the C_r is charged up with a more or less constant current, and so the voltage across it rises linearly. When the switch is turned on, the energy stored in the capacitor is transferred to the inductor, causing a sinusoidal current to flow in the switch. During the negative half wave, the current flows through the anti-parallel diode, so in this period there is no current through or voltage across the switch, and it can be turned off without losses [5].

2.2.2 Zero Voltage Switch(ZVS)

ZVS consists of a switch (S) in series with a diode. The C_r is connected in parallel, and the L_r is connected in series. A voltage source connected in parallel injects the energy into the system [5].

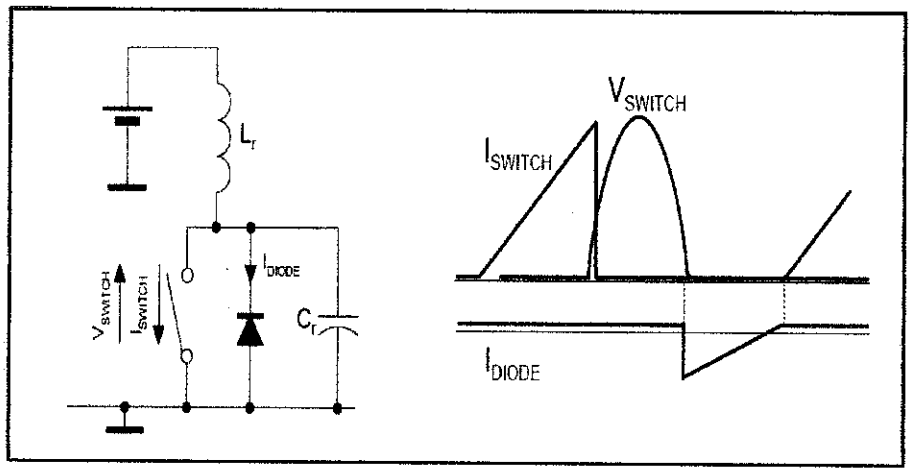

Figure 6: Full-wave zero-voltage switch - topology and waveforms

When the switch S is turned on, a linear current flows through the inductor. When the switch turns off, the energy that is stored in the inductor flows into the resonant capacitor. The resulting voltage across the capacitor and the switch is sinusoidal. The negative half-wave of the voltage is blocked by the diode. During this negative half wave, the current and voltage in the switch are zero, and so it can be turned on without losses [5].

CHAPTER 3
METHODOLOGY

3.1 Methodology

This project conducted according to this methodology to meet the objectives. Firstly, the concept and theory of resonant converter be gathered. From the research, the type of the circuit of resonant converter and its calculation of parameters are identified based on the requirement of the portable power application.

Then the project proceed with the modelling and simulation of the parameters using Pspice tools. Analyze the result and for the final stage, the circuit designed. Figure 7 shows the simplified methodology.

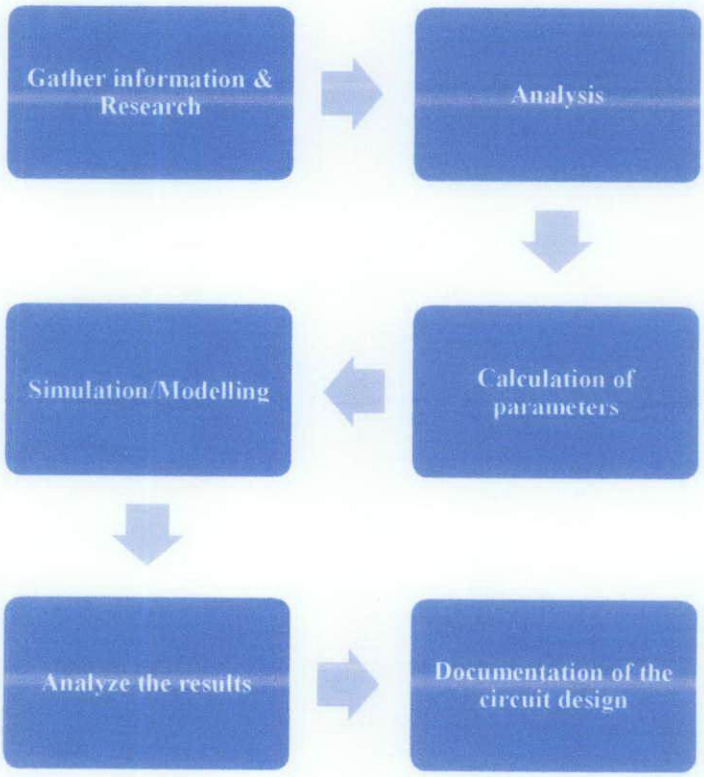

Figure 7 : Flow chart of methodology

3.2 Project Planning

Details/Week	1	2	3	4	5	6	7	8	9	10	11	12	13	14
Proposing the topic														
Information gathering														
Extended proposal submission														
Analysis														
Calculation of parameters														
Simulation/Modelling														
Proposal Defense														
Draft report submission														
FYP1 interim report submission														

Table 1 : Gantt chart for FYP1

etails/Week	1	2	3	4	5	6	7	8	9	10	11	12	13	14	15
nalyze the result															
bmission of progress report															
esign the circuit															
e-EDX															
bmission of draft report															
bmission of dissertation(soft bound)															
bmission of technical paper															
al presentation															
bmission of project dissertation (hardbound)															

Table 2 : Gantt chart for FYP2

3.3 Project Activities

3.3.1 Circuit Description

The circuit topology chosen is Parallel Resonant Converter from article [9] as shown in Figure 8 below. The values of L_r, C_r, L_f, and C_f are remained the same from the original circuit.

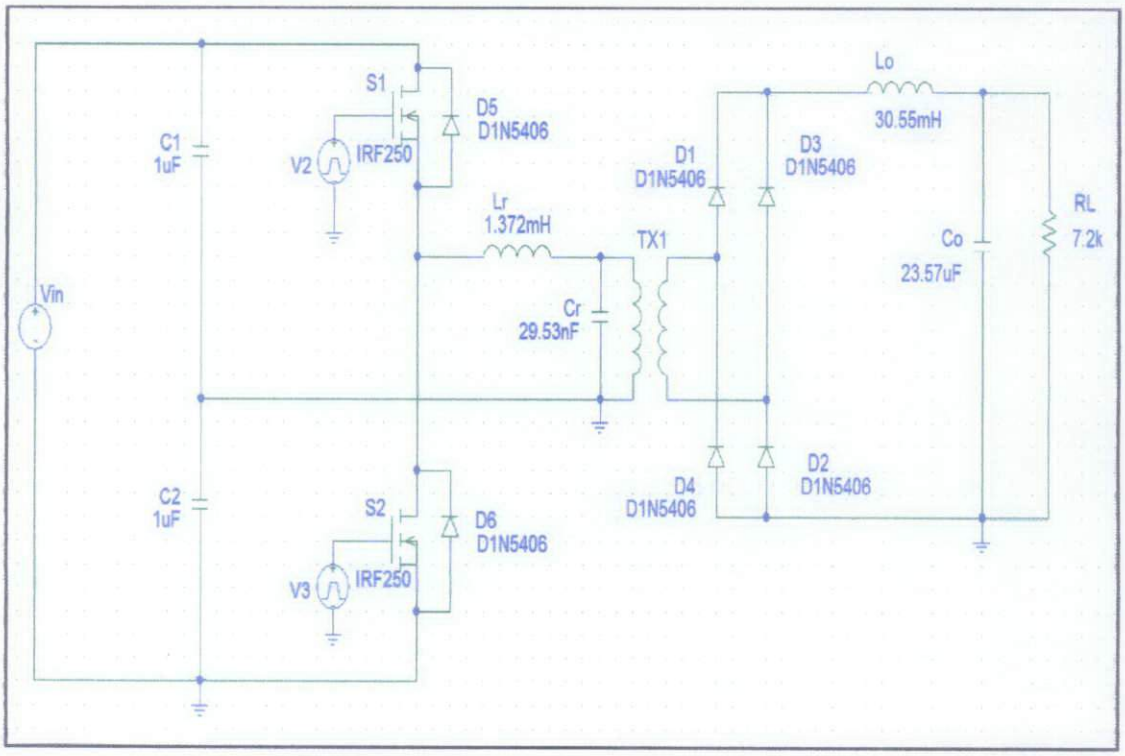

Figure 8: Parallel Resonant Converter Circuit

Mode A (Turn off of S1)

When switch S1 is turned off, at $t = T_s$ ($T_s = ½*f_s$, where f_s = triggering frequency above the resonant frequency), current is transferred to D2 from S1. Turn off losses are present in such type of operation because during turn off current and voltage are simultaneously present at the switch [9].

Mode B (Turn on of S1)

Assuming that diode D1 is conducting initially. When the current through D1 reaches zero, S1 is turned on and the current is transferred to it from the adjacent diode D1. A resonating current flows through the switch into the supply via the resonating components L_r and C_p. there is no voltage across the switch at turn on, since D1 is conducting, which eliminates turn on losses [9].

- Voltage supply

  The power supply needs to be in DC as well as the output. For this project, 340V, 272V, 204V, 136V and 66V power source values are chosen. The value is reduced for every 20%.

- MOSFET

  MOSFET IRF250 N-type is chosen for this project. MOSFET has a resistive behavior in its on state, and the output characteristic passes through zero. It can conduct a small current with a very low voltage drop [5].

- Inductor

  Lower inductor values is needed since the peak to peak current increases linearly with switching frequency chosen for high frequency converter [7].

- Capacitor

  Capacitor used to reduce voltage ripple, minimize output noise voltage and to guarantee regulation during transient loads [7].

- Diode

  Type of diode used in the simulation is D1N5406. Diode DS1 and DS2 (labeled as D5 and D6 respectively) is needed to improve switching transitions/improve switching losses

- Pulse generator setting in simulator.

  The value for pulse generator setting is different for each frequency. The setting is shown the Table 3.

	25 kHz		40 kHz		100 kHz	
	S1	S2	S1	S2	S1	S2
V1	0	0	0	0	0	0
V2	240	240	240	240	240	240
TD	0	15us	0	12.5us	0	5us
TR	2us	2us	2us	2us	1us	1us
TF	2us	2us	2us	2us	1us	1us
PW	10us	20us	8us	8us	2.5us	2.5us
PER	40us	40us	25us	25us	10us	10us

Table 3: Pulse Setting Values

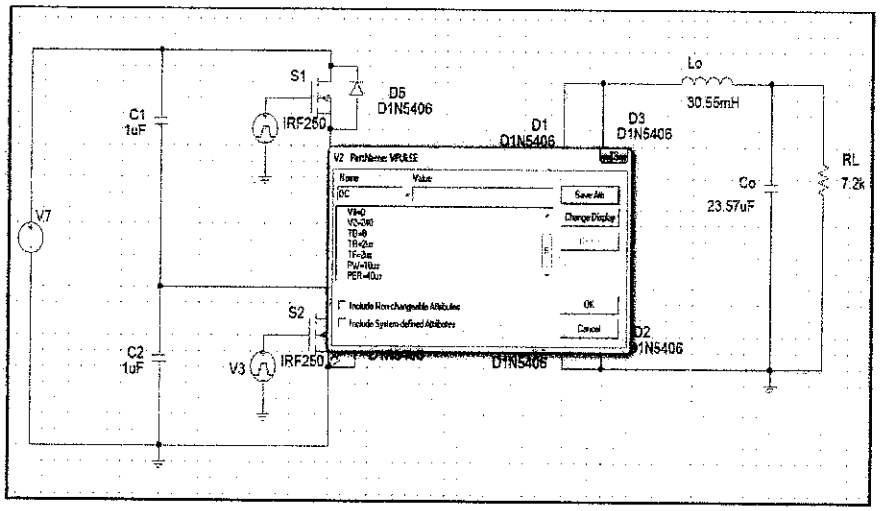

Figure 9: Pulse Setting in Pspice

3.4 Software and Tools Used

At the beginning of the simulation, the software used is Pspice Student Version 9. After gone through frequent of trial, some circuit cannot be able to simulate because of the limitation of Pspice Student Version 9. This student version limits only for 10 libraries which effect many components are not available. Then, for next simulation, Pspice Student Version do not be used anymore and proceed with Microsim 8 which able to add in libraries more than 10.

CHAPTER 4

RESULTS

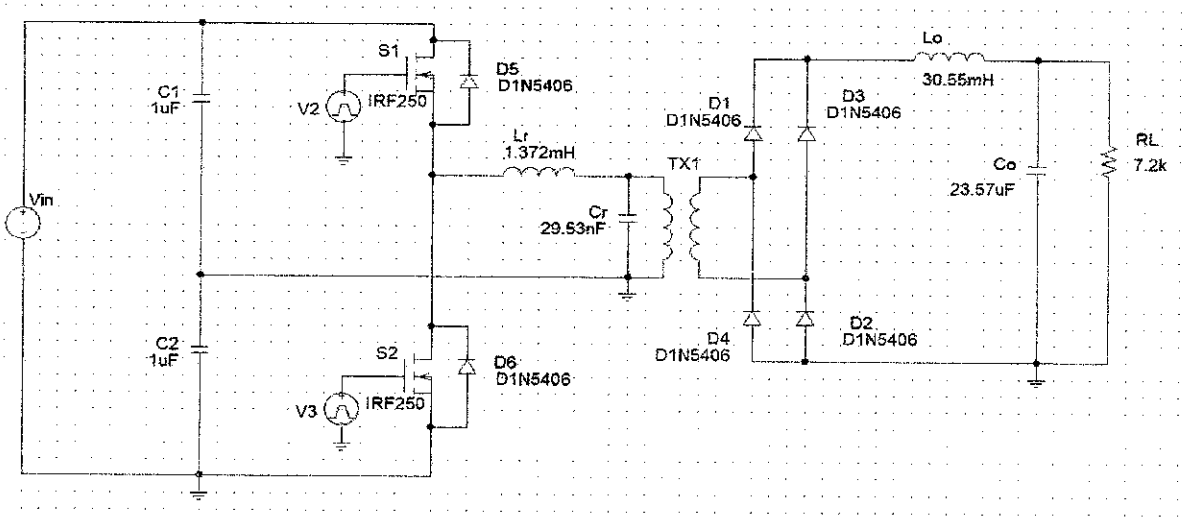

Figure 10: Parallel Resonant Converter

Fs = 40 kHz

	V (Lr)	V (TX)	V (RL)	VG (S1)	VG (S2)
340	235.658	176.001	17.703	240	240
272	187.750	140.310	14.064	192	192
204	139.808	103.112	10.437	144	144
136	68.304	91.813	6.8132	96	96
66	42.520	31.261	3.1325	47	47

Table 4 : Voltages for 40 kHz

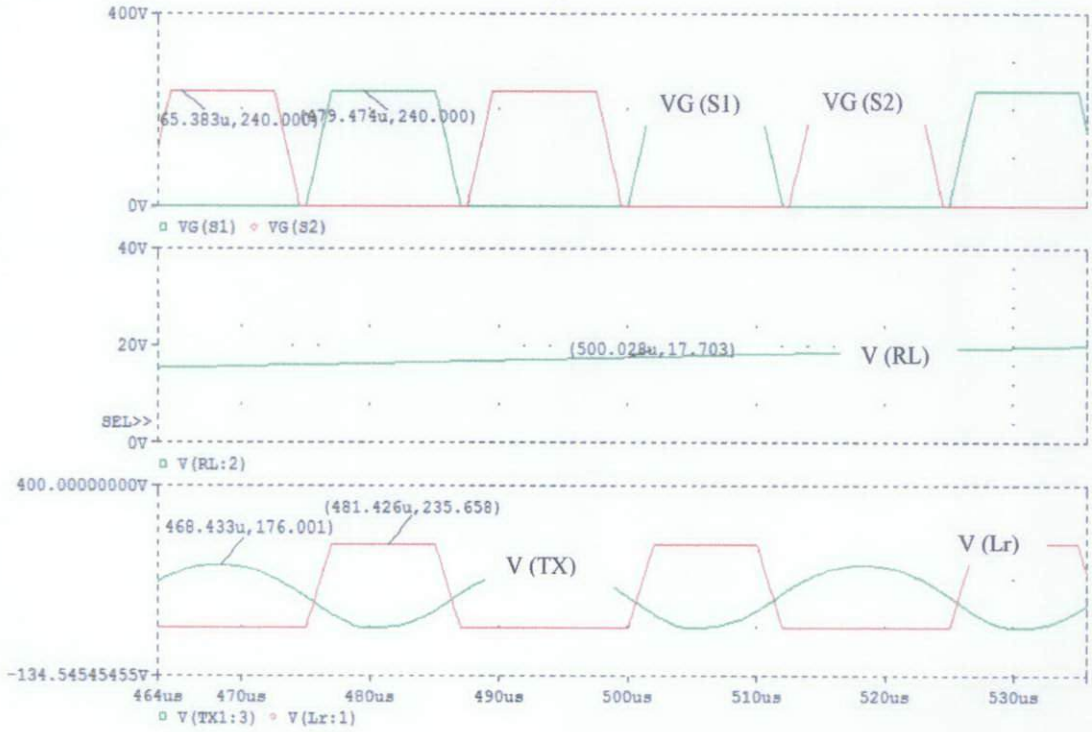

Figure 11: VG (S1), VG (S2), V (RL), V (TX), V (Lr) for 340V at 40 kHz

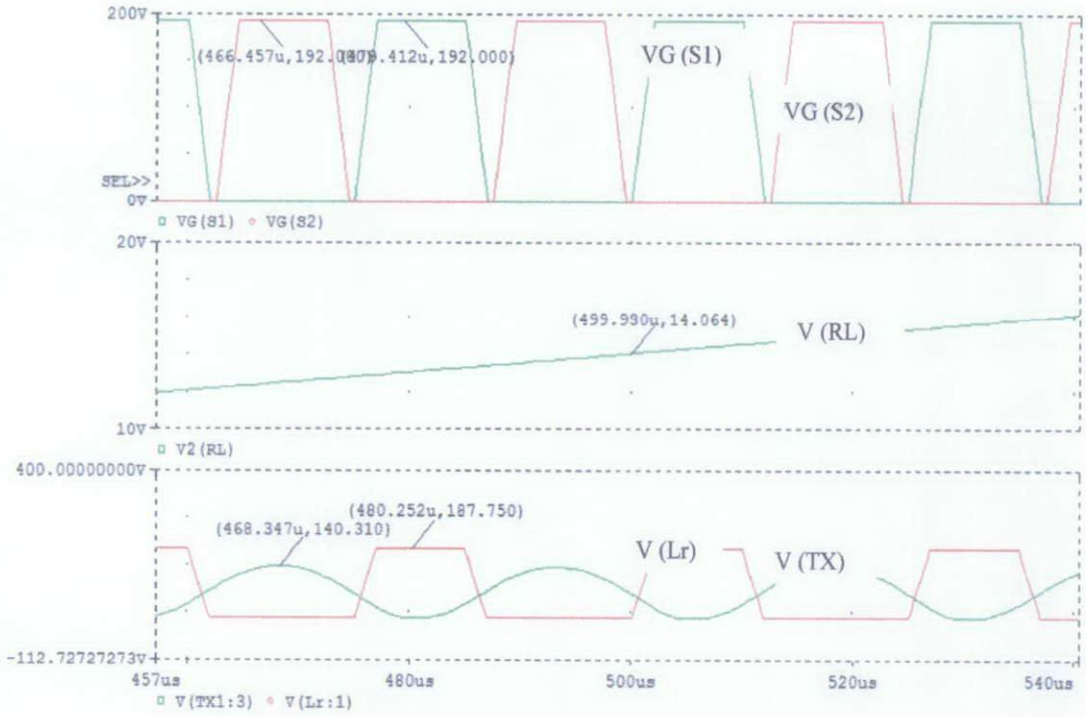

Figure 12: VG (S1), VG (S2), V (RL), V (TX), V (Lr) for 272V at 40 kHz

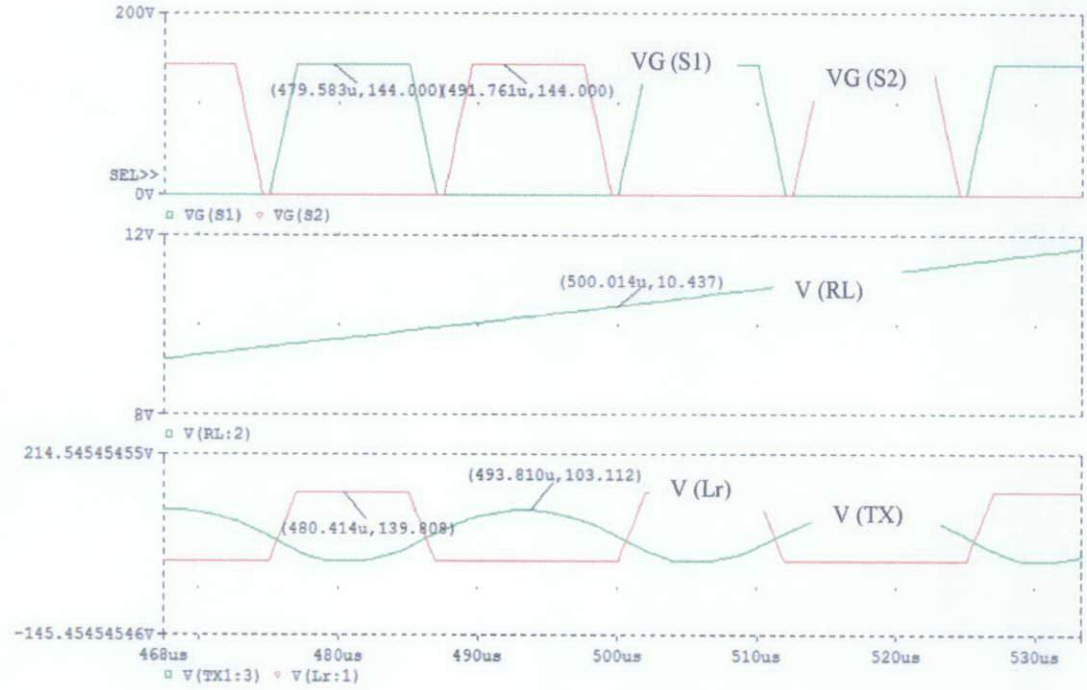

Figure 13: VG (S1), VG (S2), V (RL), V (TX), V (Lr) for 204V at 40 kHz

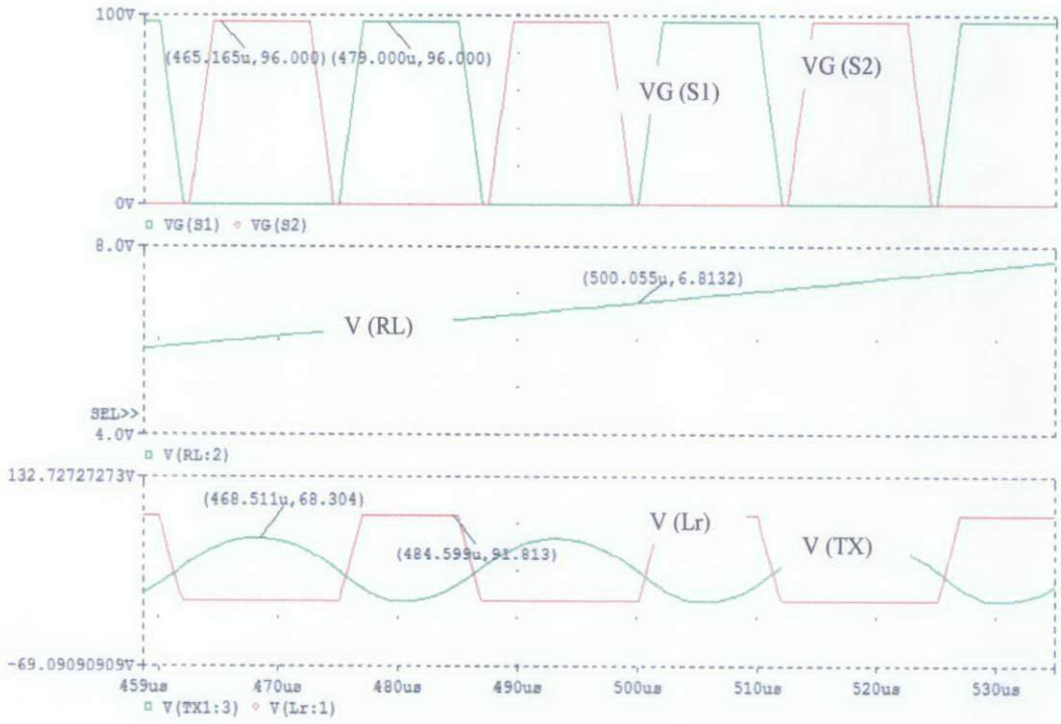

Figure 14: VG (S1), VG (S2), V (RL), V (TX), V (Lr) for 136V at 40 kHz

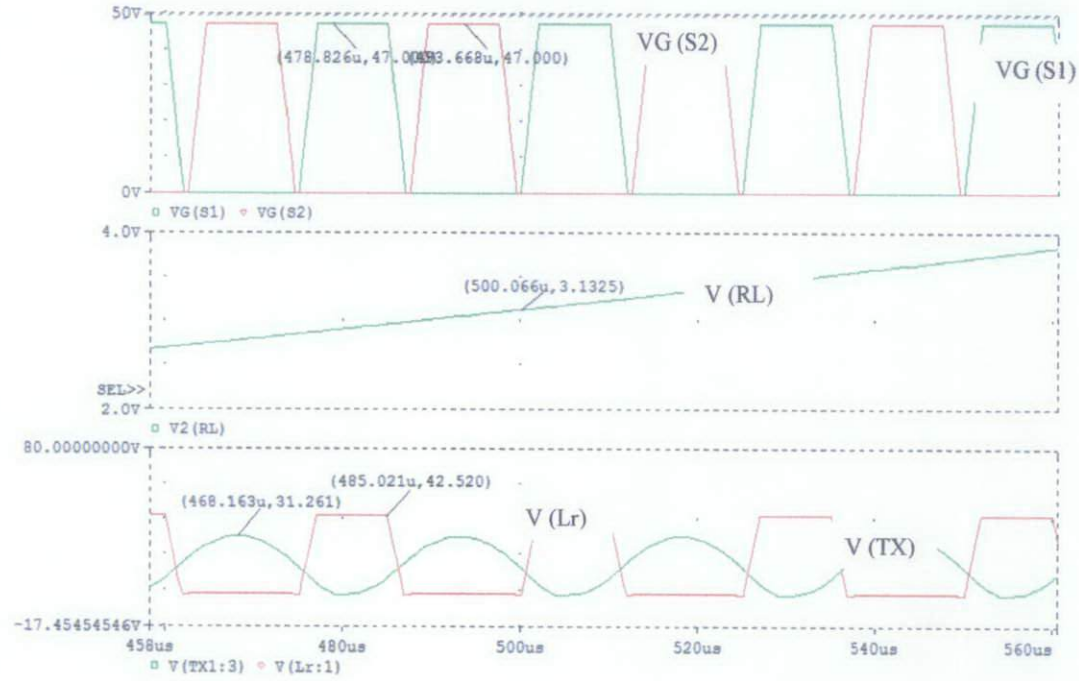

Figure 15: VG (S1), VG (S2), V (RL), V (TX), V (Lr) for 66V at 40 kHz

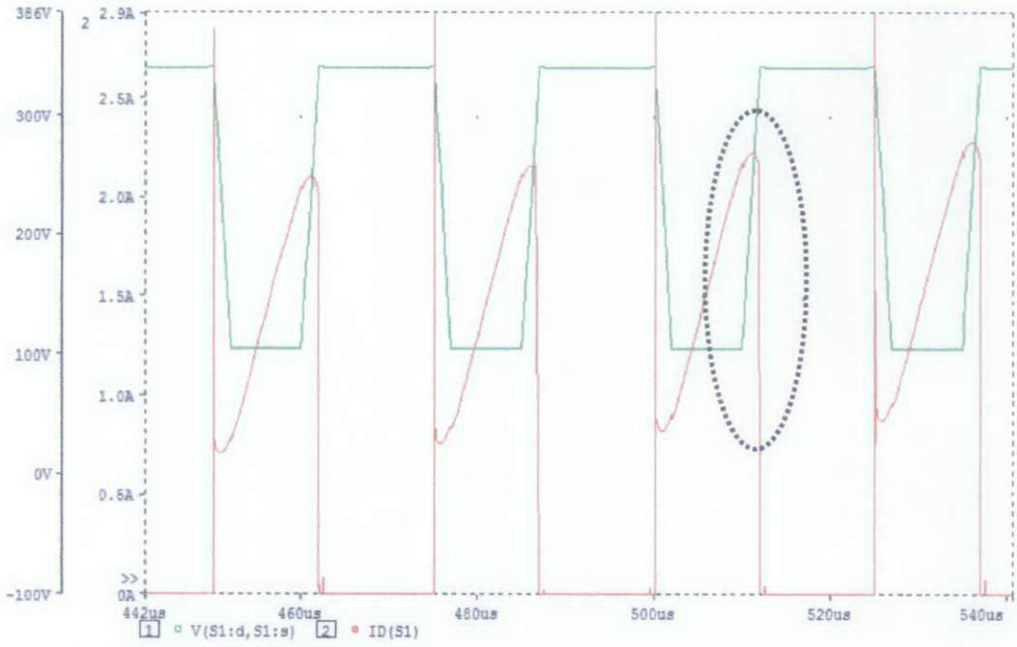

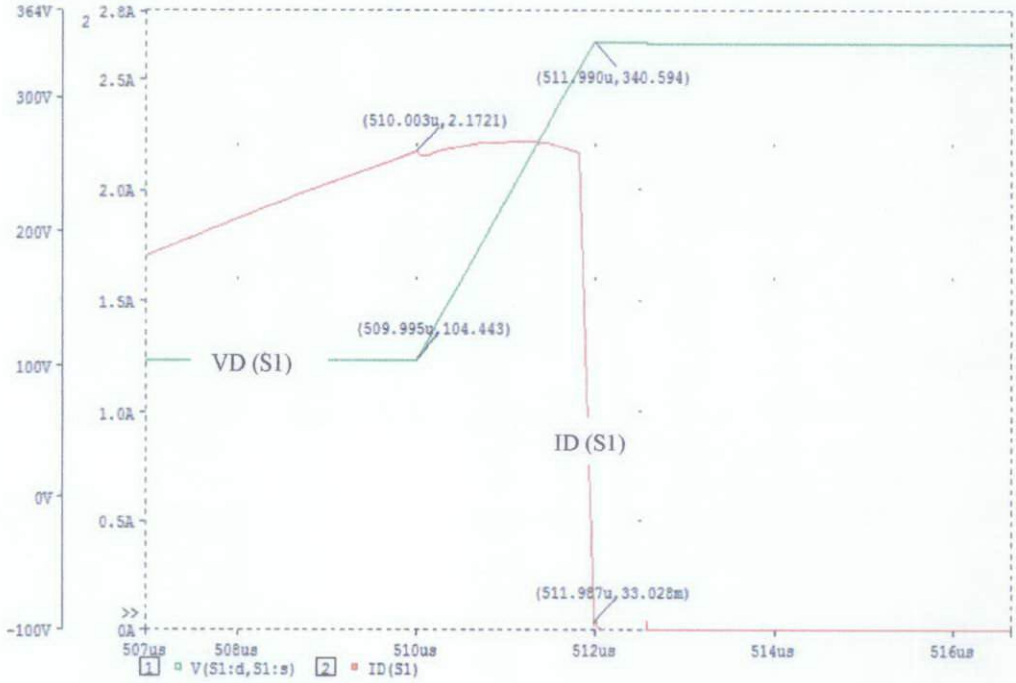

Figure 16: Switching losses at S1 (40 kHz)

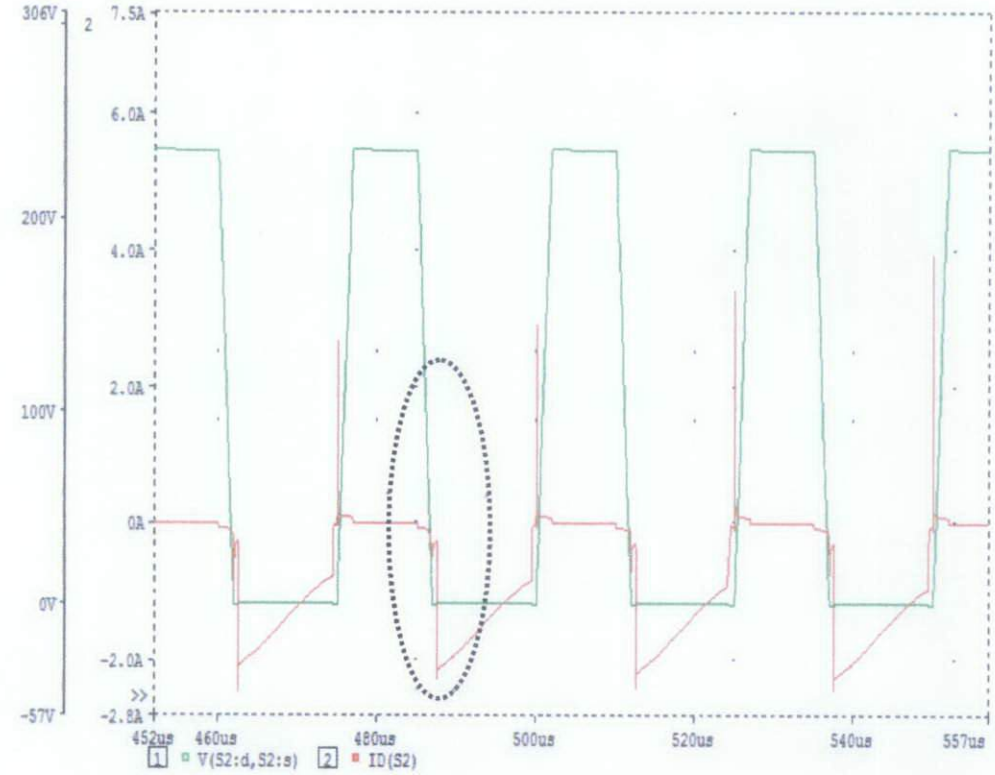

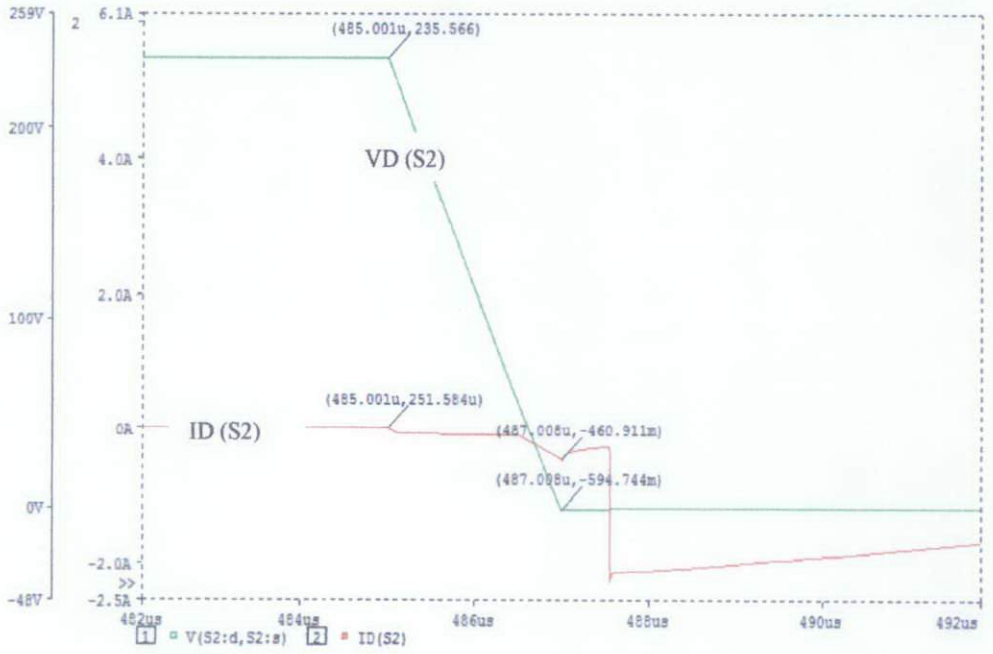

Figure 17: Switching losses at S2 (40 kHz)

Fs = 25 kHz

	V (Lr)	V (TX)	V (RL)	VG (S1)	VG (S2)
340	235.702	204.635	22.011	240	240
272	187.760	168.409	17.505	192	192
204	139.905	121.808	12.945	144	144
136	91.860	79.047	8.5001	96	96
66	42.972	38.348	3.9048	47	47

Table 5 : Voltages for 25 kHz

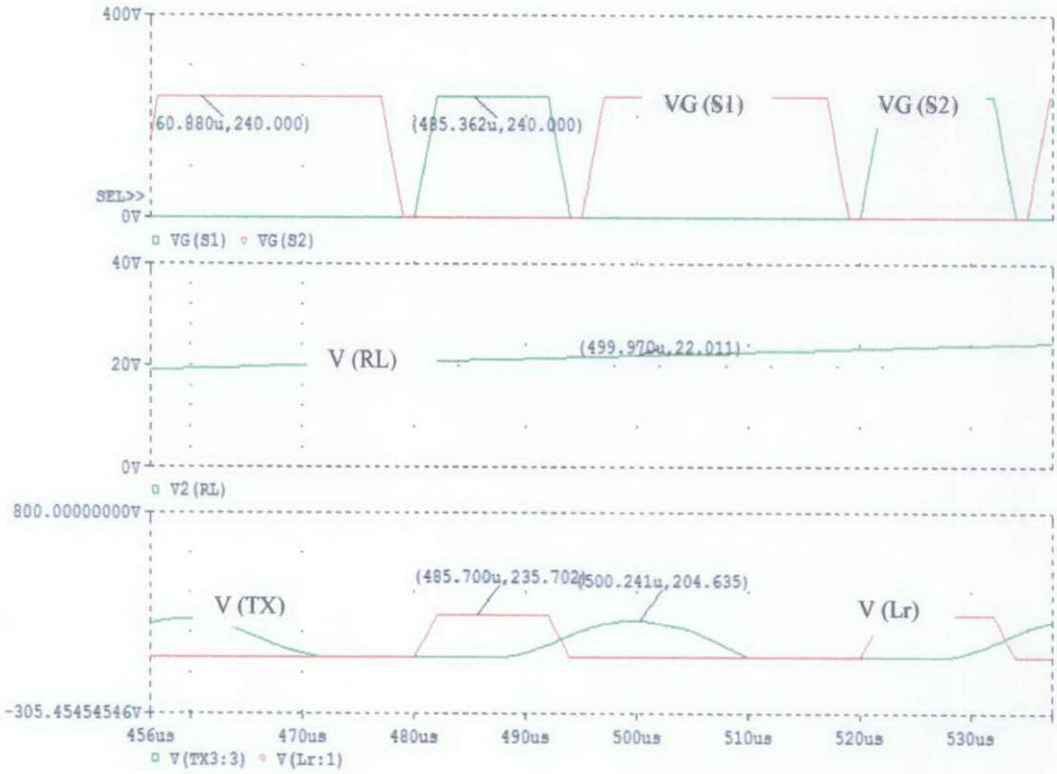

Figure 18: VG (S1), VG (S2), V (RL), V (TX), V (Lr) for 340V at 25 kHz

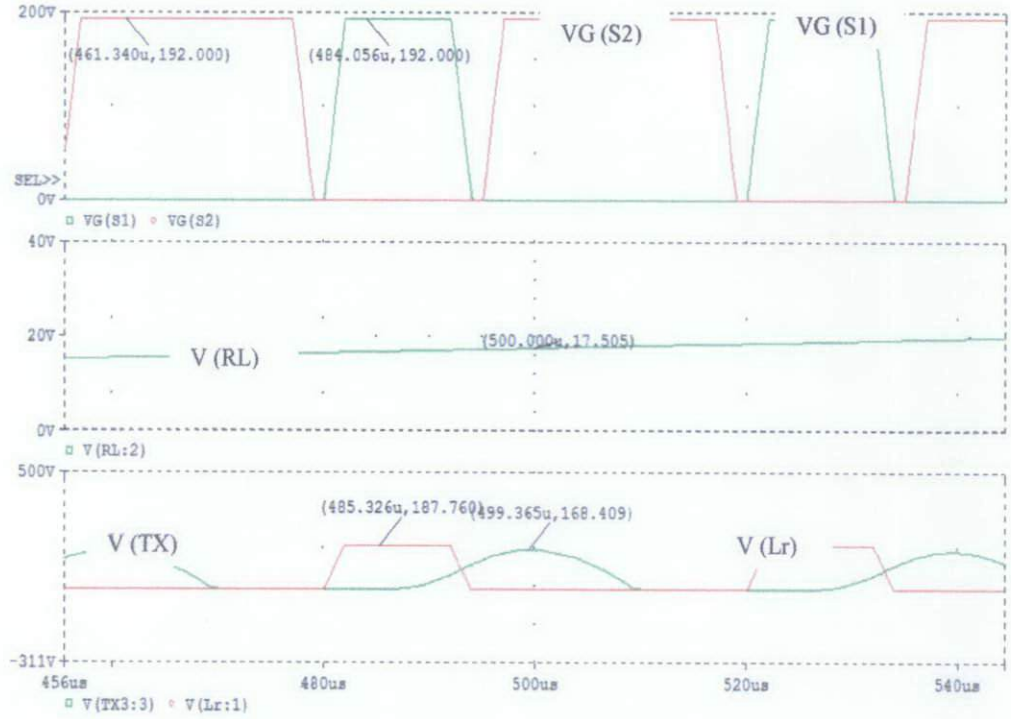

Figure 19: VG (S1), VG (S2), V (RL), V (TX), V (Lr) for 272V at 25 kHz

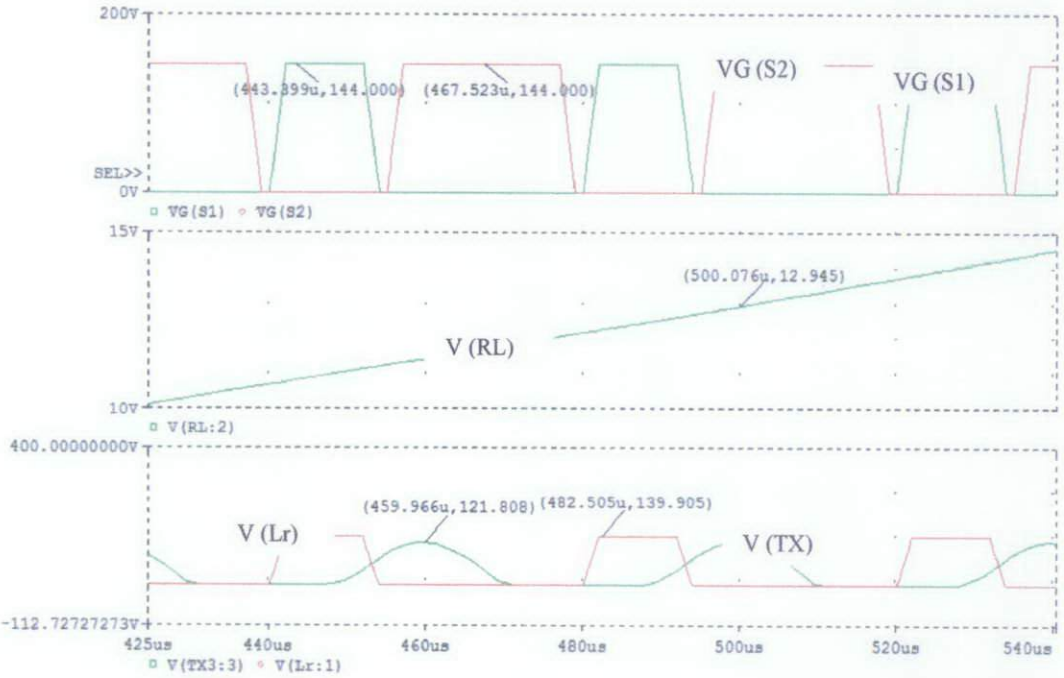

Figure 20: VG (S1), VG (S2), V (RL), V (TX), V (Lr) for 204V at 25 kHz

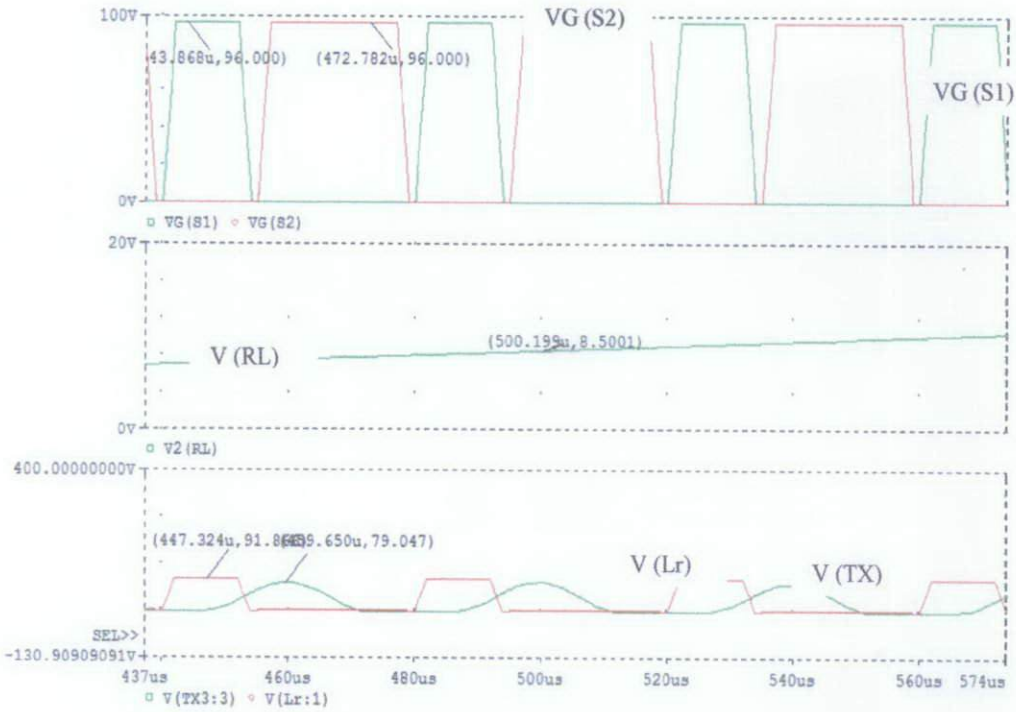

Figure 21: VG (S1), VG (S2), V (RL), V (TX), V (Lr) for 136V at 25 kHz

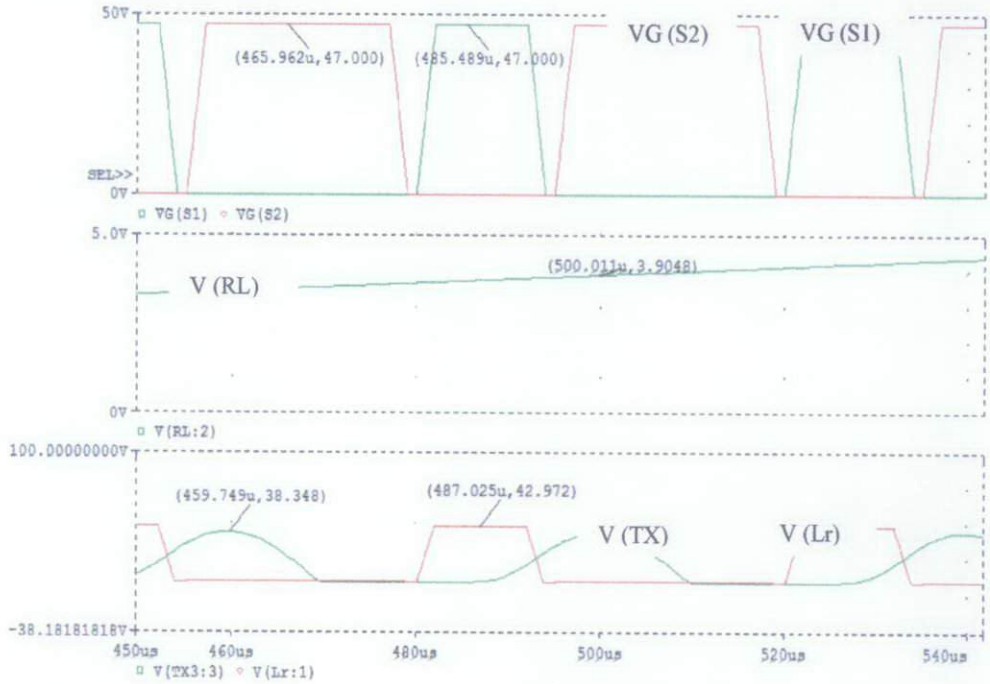

Figure 22: VG (S1), VG (S2), V (RL), V (TX), V (Lr) for 66V at 25 kHz

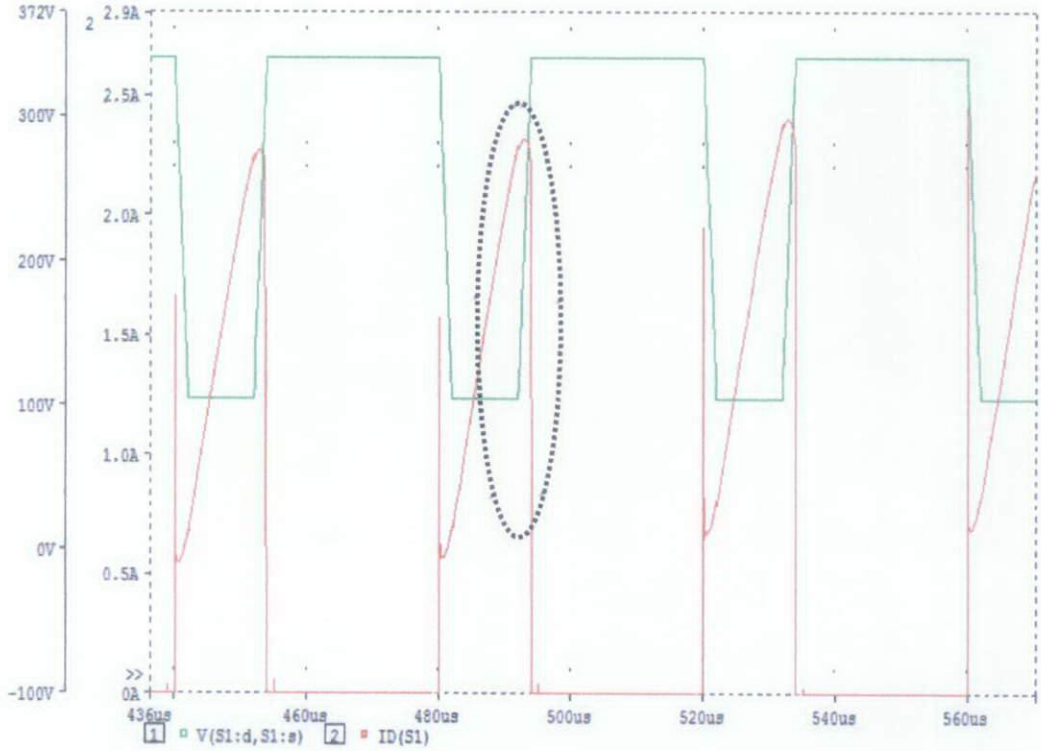

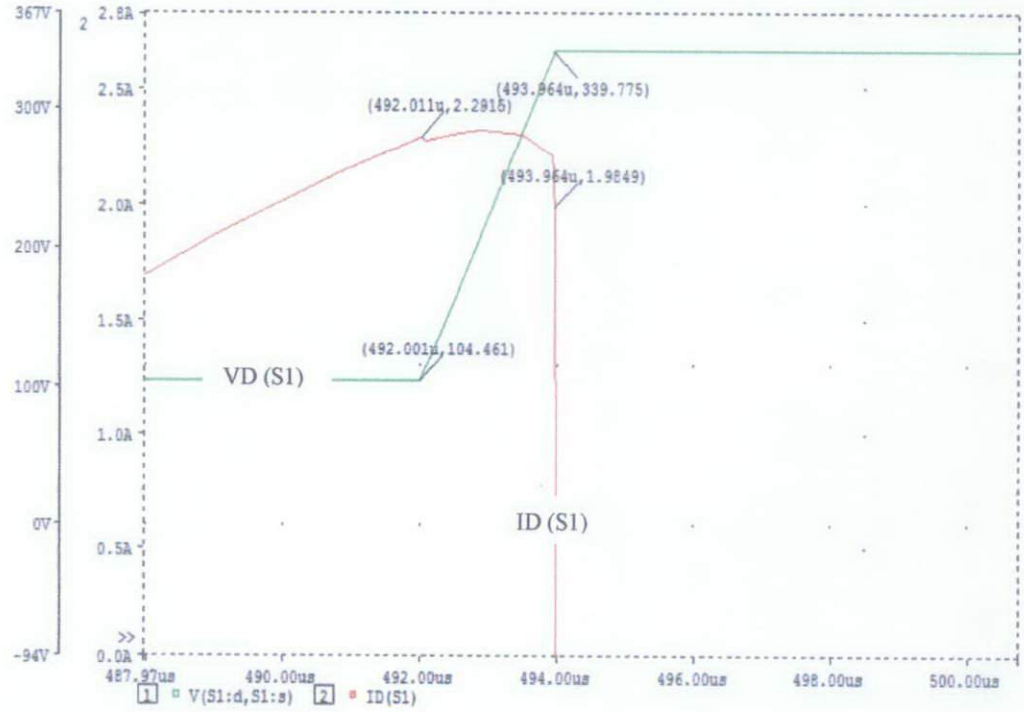

Figure 23: Switching losses at S1 (25 kHz)

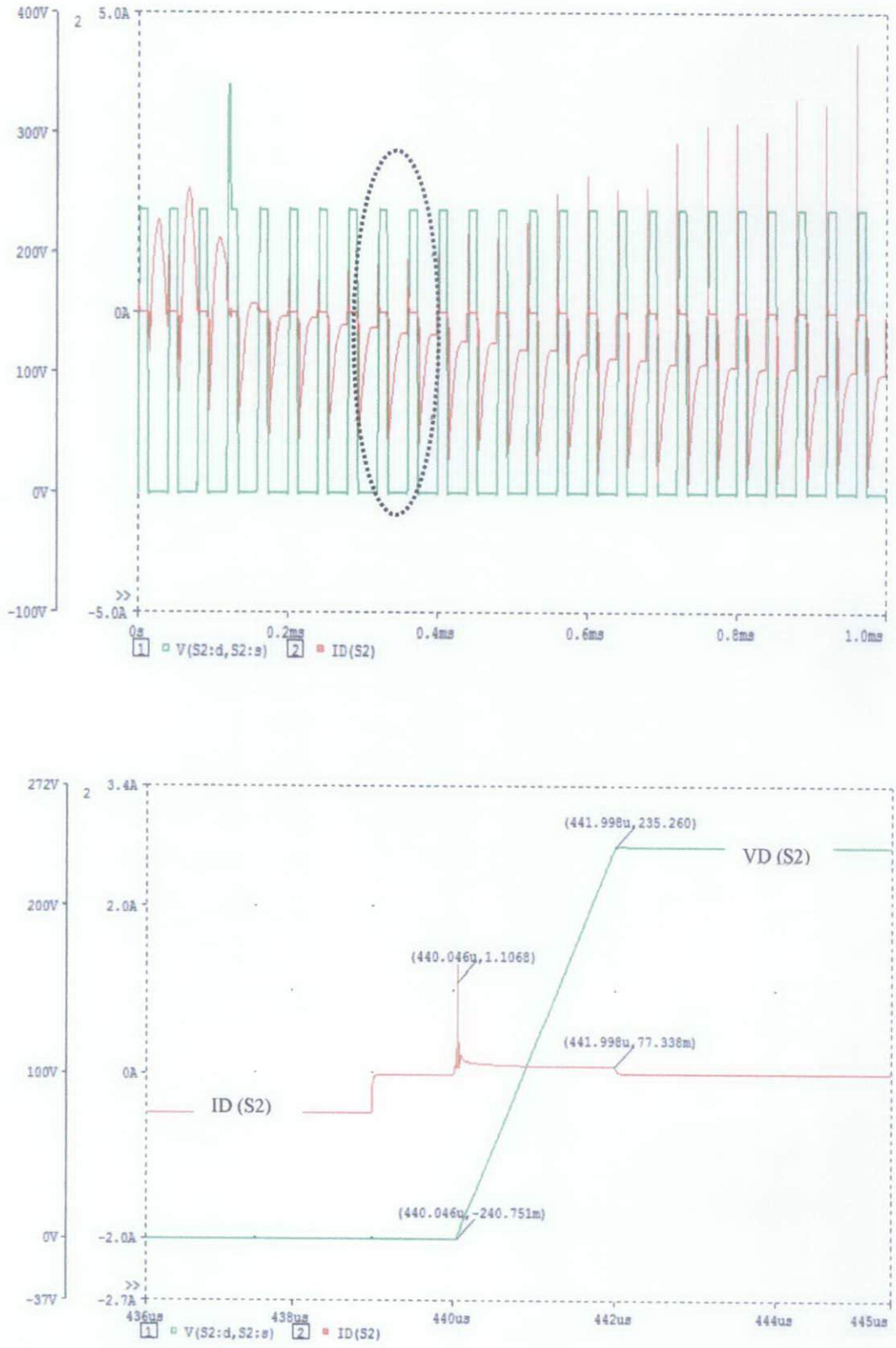

Figure 24: Switching losses at S2 (25 kHz)

Fs = 100 kHz

	V (Lr)	V (TX)	V (RL)	VG (S1)	VG (S2)
340	235.728	91.461	13.699	240	240
272	187.778	73.706	10.866	192	192
204	139.845	55.383	8.0403	144	144
136	91.897	37.288	5.2163	96	96
66	43.003	16.646	2.3481	47	47

Table 6 : Voltages for 100 kHz

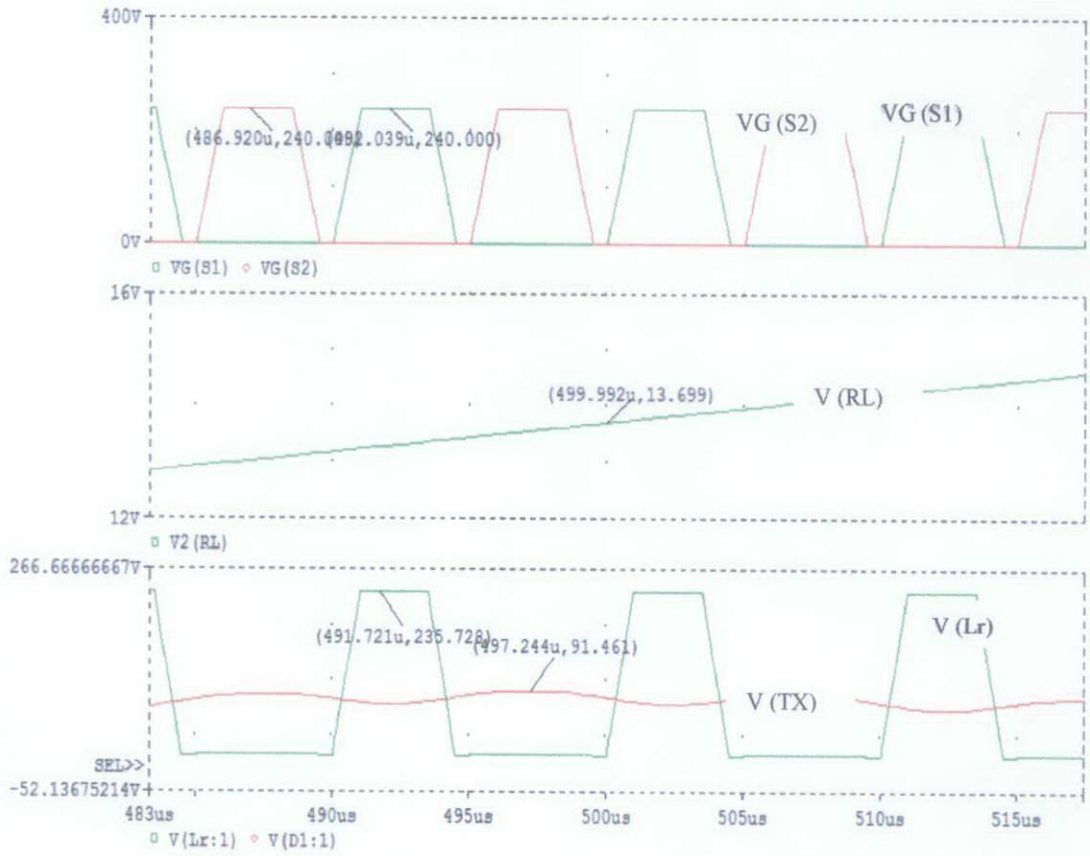

Figure 25: VG (S1), VG (S2), V (RL), V (TX), V (Lr) for 340V at 100 kHz

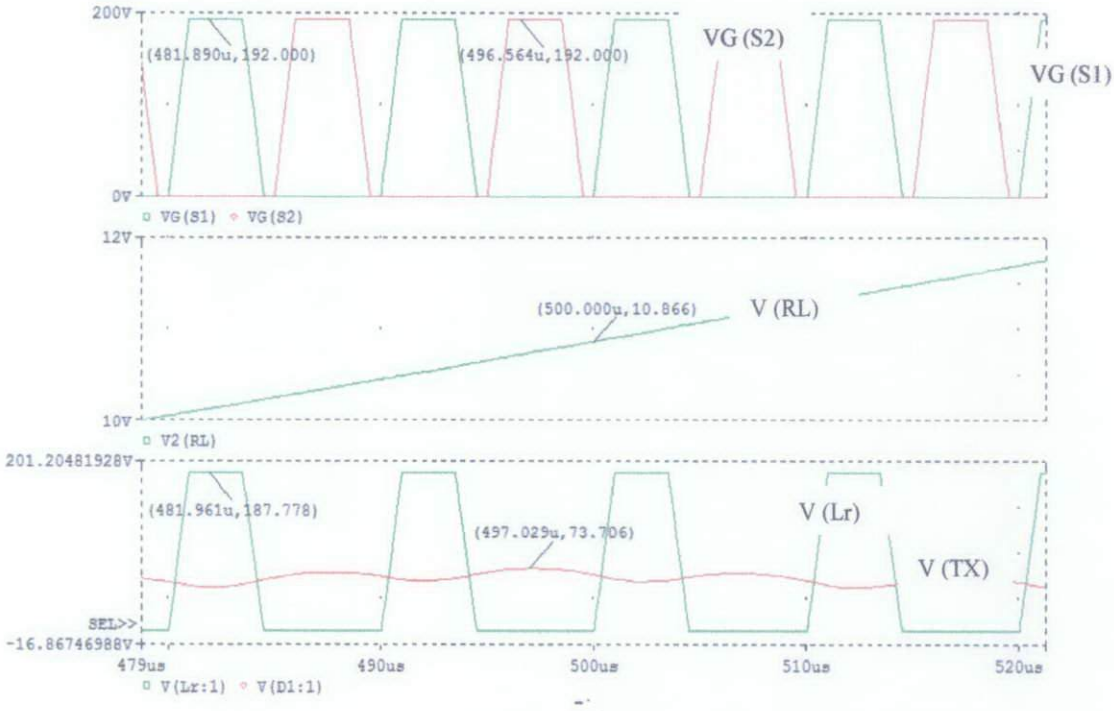

Figure 26: VG (S1), VG (S2), V (RL), V (TX), V (Lr) for 272V at 100 kHz

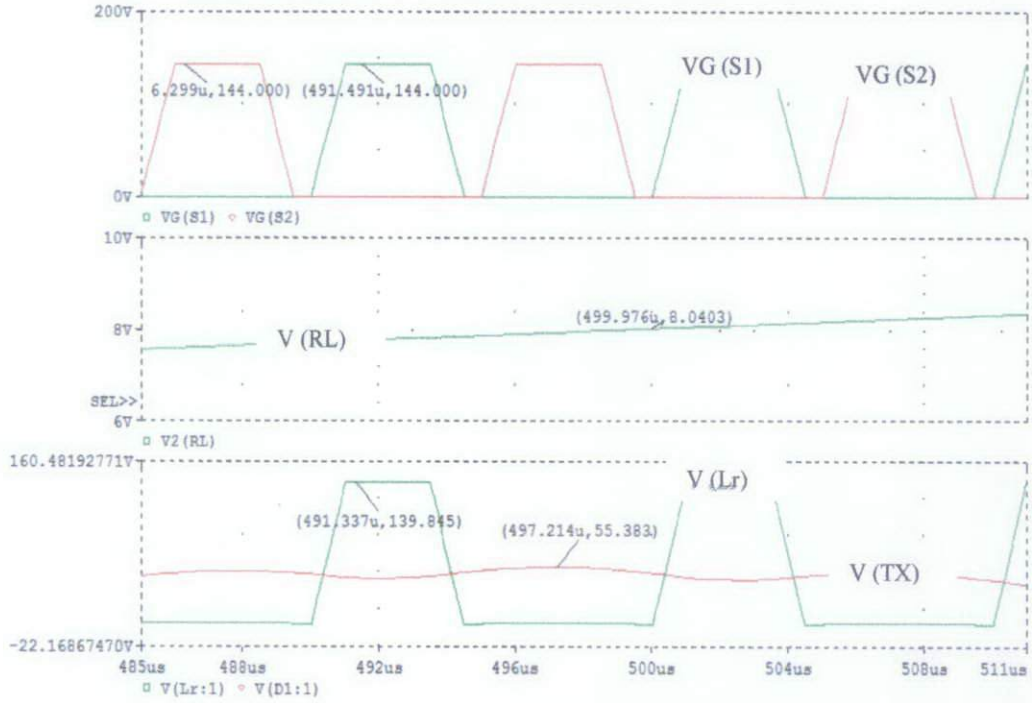

Figure 27: VG (S1), VG (S2), V (RL), V (TX), V (Lr) for 204V at 100 kHz

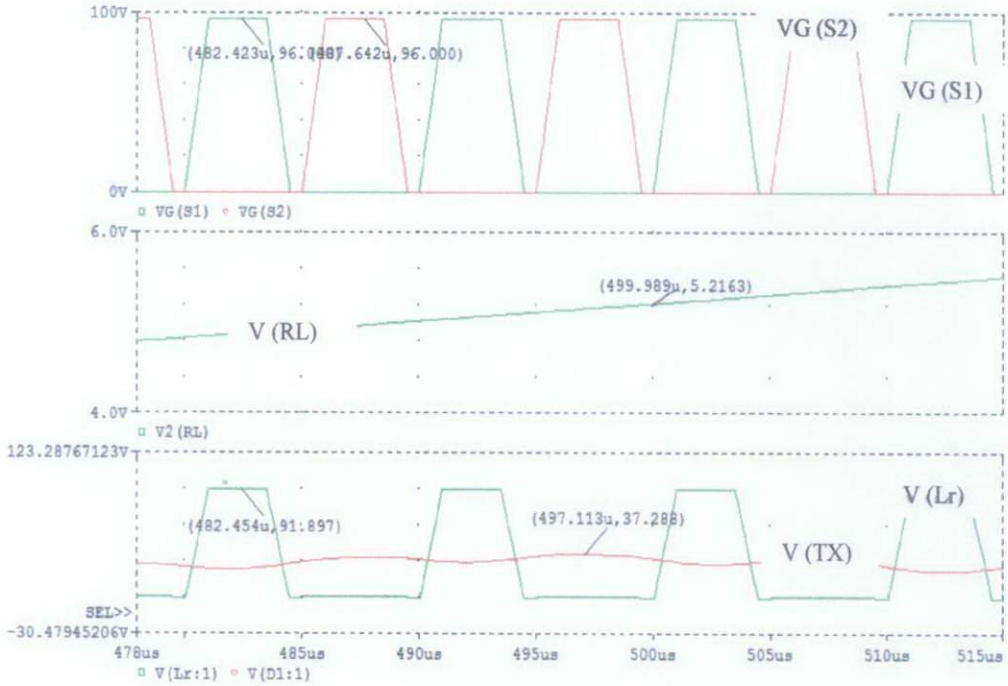

Figure 28: VG (S1), VG (S2), V (RL), V (TX), V (Lr) for 136V at 100 kHz

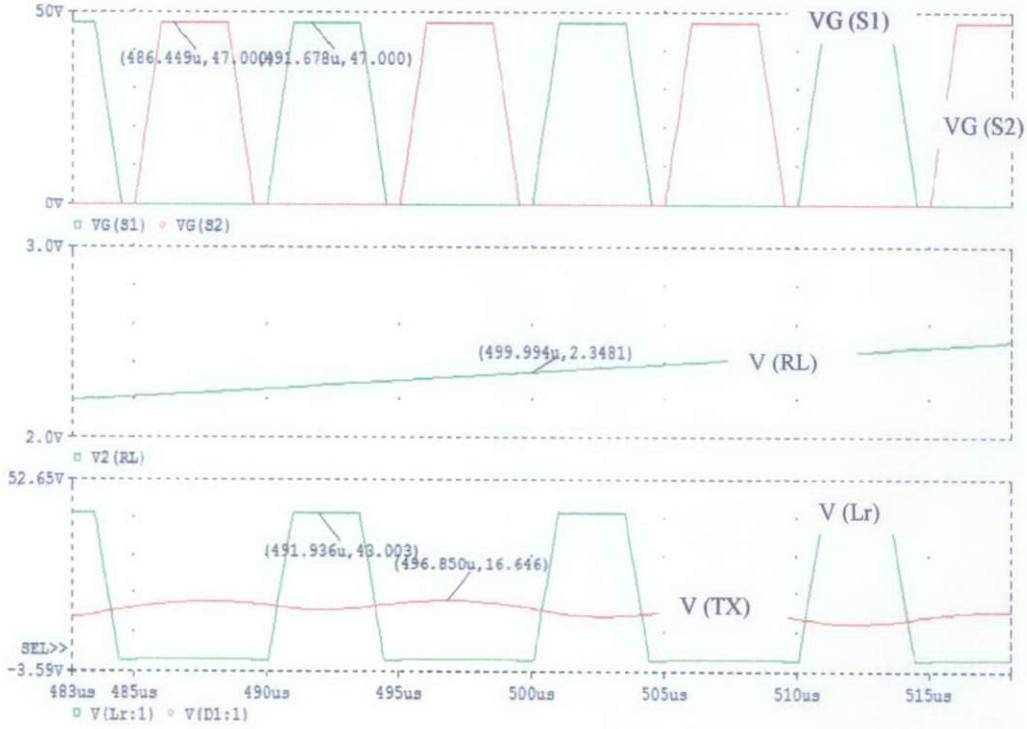

Figure 29: VG (S1), VG (S2), V (RL), V (TX), V (Lr) for 66V at 100 kHz

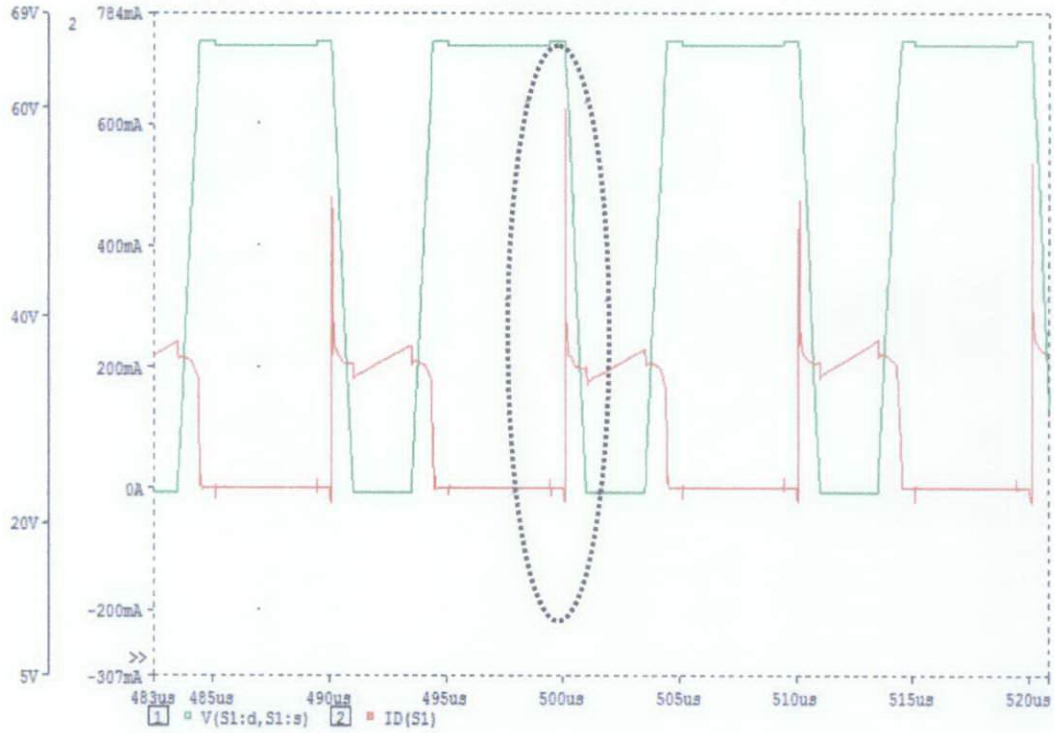

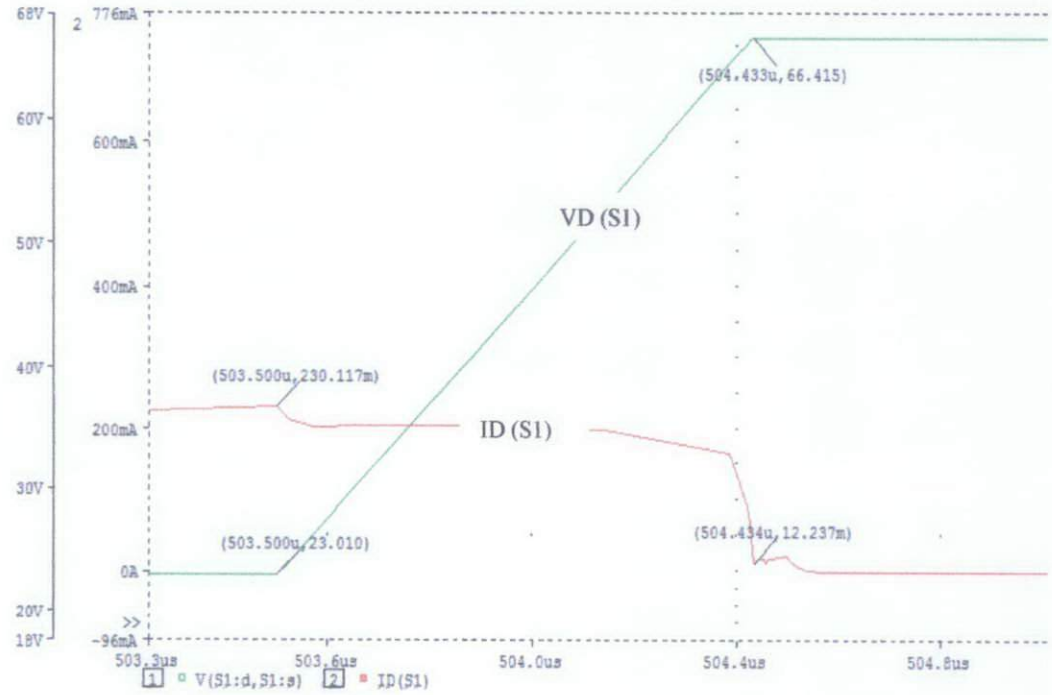

Figure 30: Switching losses at S1 (100 kHz)

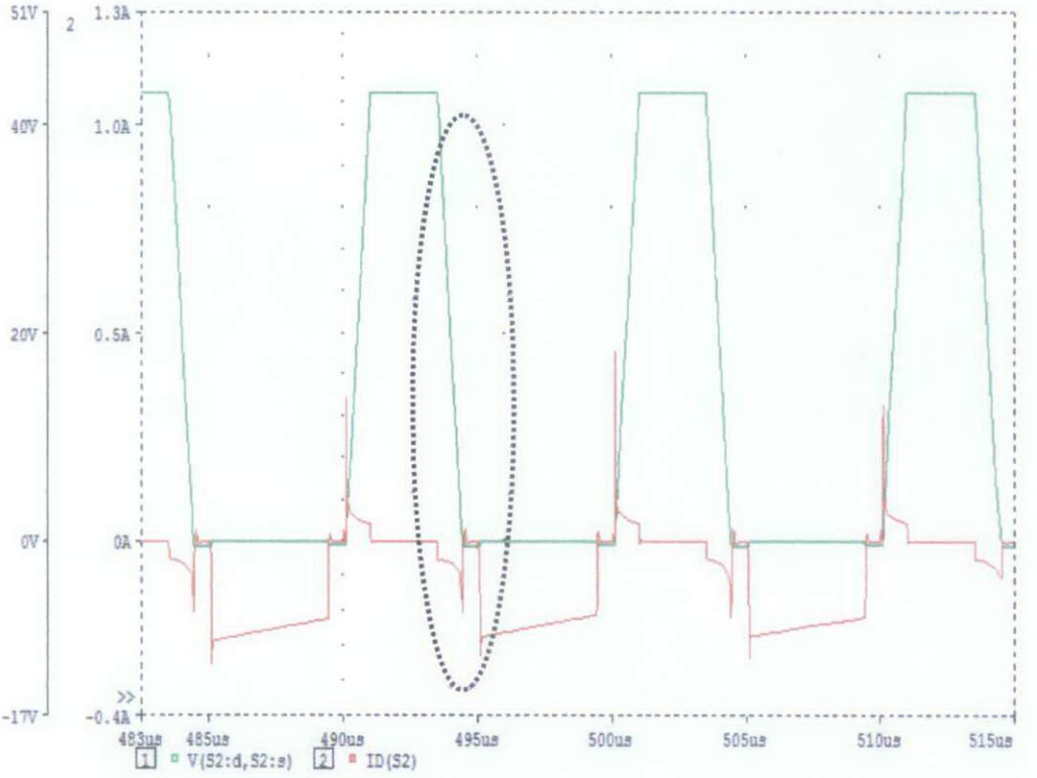

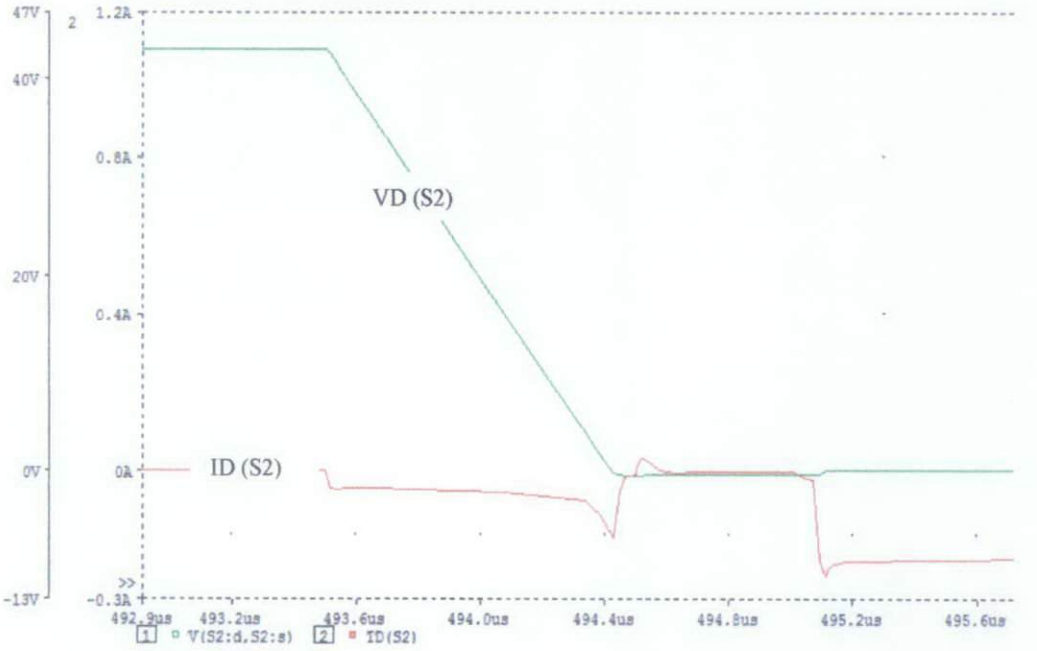

Figure 31: Switching losses at S2 (100 kHz)

The resonant frequency for this circuit is f_r = 25 kHz. Based on the equation (2)

$$fr = \frac{1}{2\pi\sqrt{L_r C_r}} = \frac{1}{2\pi\sqrt{(1.372m)(29.53n)}} = 25\ kHz$$

The switching frequencies are 25 kHz (at resonance), 40 kHz (slightly above resonance), and 100 kHz (high above resonance). Calculation of switching frequency is based on equation (1)

$$f_s = \frac{1}{T_s} = \frac{1}{40us\ @\ 25us\ @\ 10us} = 25kHz@40kHz@100kHz$$

For Fs = 40 kHz, the voltage at V (Lr) is higher than at V (TX). The voltage drop after go through the resonant components, L_r and C_r. The voltage at load resistance,R_L decreasing as voltage supply decreasing for every 20%. The voltage value for resistance load is taken at time simulation t=500us.

The voltage value for resonant inductor, V (L_r) is mostly in the same range when the comparison is made with other value of frequencies. There is a bit different in voltage at transformer, V (TX). When the frequency is increasing from 25 kHz to 100 kHz, the V (TX) is decreasing.

The switching losses at S1and S2 are calculated using the formula below.

$$P_{sw} = \frac{1}{2} t_{sw} P_{peak} f_{sw} \qquad (6)$$

For Fs = 40 kHz

$P_{SW}(S1)$ = 1/2 (511.987u-509.995u) (2.25A*250V) (40 kHz) = 22.41W

$P_{SW}(S2)$ = undefined since voltage and current is not well intercept.

For Fs = 25 kHz

$P_{SW}(S1)$ = 1/2 (493.964u-492.001u) (2.25A*280V) (25 kHz) = 15.46W

$P_{SW}(S2)$ = 1/2 (441.998u-440.046u) (77.338mA*100V) (25 kHz) = 0.19W

For 100 kHz

$P_{SW}(S1)$ = 1/2 (504.433u-503.500u) (200mA*35V) (100 kHz) = 0.33W

$P_{SW}(S2)$ = 0 since the area under the graph of voltage and current is zero.

The simulated switching losses graph is compared to the ideal switching losses graph as shown in Figure 30.

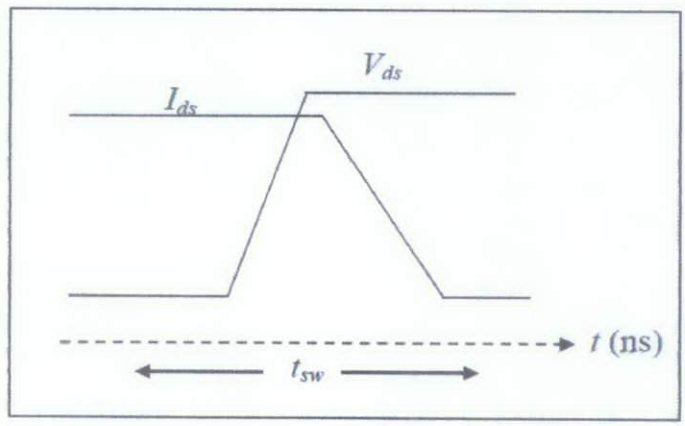

Figure 30: Ideal V-I switching loss

Based on the calculation, the best switching losses is at Fs = 100 kHz. The switching losses at S1 are less than 1 and for S2 is 0. Although the voltage resistance load at 100 kHz is lower than 25 kHz during t=500us, the voltage is still sufficient for portable application.

CHAPTER 5

CONCLUSIONS

- The best frequency for the parallel resonant converter to operate is at above resonance Fs = 100 kHz.

- The switching losses is smallest at fs = 100 kHz.

- It is recommended for this project to change the resonant frequency by changing the values of Lr and Cr values and increase the switching frequency until 1MHz.

REFERENCES

[1] "Chapter 19 Resonant Conversion" Fundamentals of Power Electronics Circuits

[2] Young-Goo Kang, Anand K.Upadhyay, "Analysis and Design of a Half-Bridge Parallel Resonant Converter" *in IEEE Transactions on Power Electronics*, July 1988

[3] Biju S. Nathan, V. Ramanarayanan, "Analysis, Simulation and Design of Series Resonant Converter for High Voltage Applications" *in IEEE*, 2000

[4] O.A. Eno, D.S. Thompson,J. Coppin, "High Power Resonant Topology For dc-dc Converter" *in EPE*, 2005

[5] M. Bildgen, "Resonant Converter Topologies" *Application STMicroelectronics*, 1999

[6] Peter Markowski, "Estimating MOSFET switching losses means higher performance buck converters" *Artesyn Technologies*, December 2002

[7] A. K. Panda, Aroul. K, "A Novel Technique to Reduce the Switching Losses in a Synchronous Buck Converter", *International Conference on Power electronics,drives and Energy System, PEDES*, December 2006

[8] Ying-Chun Chuang, Yu-Lung Ke, Shun-Yi Chang, "Highly-Efficient Battery Chargers with Parallel-Loaded Resonant Converters", *IEEE*, 2009

[9] Unknown, " Chapter 2: Theory PRC Circuit"

[10] Muhammad H. Rashid, " Introduction to Pspice Using Orchad for Circuits and Electronics", *3rd edition Pearson Prentice Hall*, 2004

[11] Igor Korotyeyev,Valeri Zhuikov,Radoslaw Kasperek, " Electronical System Calculation and Analysis with Mathematica and Pspice" *CRC Press*

[12] Issa Batarseh, "Power Electronic Circuits" *John Wiley & Sons*,2004

[13] P. Si, A. P. Hu, J. W. Hsu, M. Chiang, Y. Wang, S. Malpa, D. Budgett, "Wireless Power Supply for Implantable Biomedical Device Based on Primary Input Voltage Regulation",*IEEE*

[14] R. W. Erickson, "Chapter 19: Resonant Conversion", *Fundamentals of Power Electronics*, 2nd ed. Kluwer Academic Publisher, 2001, pp. 709-713.

[ighly-Efficient Battery Chargers with Parallel-Loaded Resonant Converters

Ying-Chun Chuang **Yu-Lung Ke** **Shun-Yi Chang**

mail:chuang@mail.ksu.edu.tw e-mail:yulungke@ms25.hinet.net e-mail:nickelayu@hotmail.com

Department of Electrical Engineering, Kun Shan University, Tainan Hsien 71003, Taiwan, R.O.C.

t—The well established advantages of resonant converters tery chargers, including fast response, low switching easy of the control scheme, simplicity of circuit ration, and low electromagnetic interference (EMI), others, have led to their increasing attraction. This work s a highly efficient battery charger with a parallel-loaded t converter for battery charging applications to improve formance of traditional switching-mode charger circuits. irging voltage can be regulated by varying the switching cy. The switching frequency of the parallel-loaded t battery charger was set at continuous conduction mode Circuit operation modes are determined from the ion profiles. Operating equations and operating theory) developed. This study utilizes the fundamental wave mation with a battery equivalent circuit to simplify the circuit analyses and presents an efficient, small-sized, t-effective switched-mode converter for battery chargers. otype charger with parallel-loaded resonant converter l for a 12V-48Ah battery is built and tested to verify the al predictions. The maximum charging efficiency of the d battery charger topology is as high as 90.9%. tory performance is obtained from the experimental

ls- battery charger, parallel-loaded resonant converter, soft-switching converter.

I. INTRODUCTION

eries are commonly used in renewable generation , electrical vehicles, communications systems and er systems as electrical energy storage elements [1]– hough there are many kinds of batteries that can be ie lead-acid battery can afford to store a reasonable of electrical energy and is adopted widely in the al field [8]-[11]. As the chemical reaction of the g and discharging processes of the lead-acid battery tate the electrolyte and produce hydrogen gas, this will reduction of the electrolyte and the stored-energy ty. Furthermore, the allowable usable life of the can also be reduced significantly. Therefore, a delicate d battery charging system must be used to store the l energy of the battery. How to maintain the m capacity of lead-acid battery and extend its usable n important design problem for a charger, so many charging schemes have been proposed to improve this problem. Hence, we need to develop a high performance charger circuit in a battery energy storage system (BESS) [12]-[16].

Traditionally, the charger can be classified in two categories: the linear-mode converters and the switch-mode converters [17]-[19]. The linear-mode converters offer the designer three advantages: simplicity in design, no electrical noise in the output, and low cost. While the linear-mode converter may be a simple way of converting a dc source to a lower dc voltage and charging a battery, the low efficiency of this charger circuit is a serious drawback for battery charging applications. An alternative method to improve the aforementioned problems is to employ a switch-mode converter that has the merits of high efficiency, small size and low cost. However, the switching devices consume power when they are turned on or off if they go through a transition when both voltage and current are nonzero. As the switching frequency increases, these transitions happen more often and the power loss in the device increases. To solve this problem, a new class of switch-mode converters known as soft-switching resonant converter, has been thoroughly investigated in recent years [20]. The advantages of the resonant converter include the soft switching of power switches, leading to low switching losses, which in turn result in greater charger efficiency and higher switching and operating frequency. Consequently, the size and weight of the charger are reduced. Another benefit of soft-switching resonant converters over conventional switch-mode converters is the decrease in the harmonic content in the converter voltage and current waveforms. Therefore, when the resonant converters and conventional switch-mode converters are operated at the same power level and frequency, the resonant converters can be expected to have lower EMI problems. Accordingly, resonant converters have become the crucial technology for the majority of converters to improve power density, efficiency, reliability, and other performance characteristics.

The life and capacity of the batteries depend on several factors, such as charge mode, maintenance, temperature, and age. Among these factors, the charge mode has a great impact on battery life and capacity. The batteries should be charged with current and voltage levels with low ripple. Therefore, a

978-1-4244-3476-3/09/$25.00 ©2009 IEEE

erformance battery charger is necessary in a BESS. In o minimize the power losses, it is essential not to waste in the conversion process. In relation to the power nics and associated control schemes, the main ment is to guarantee that the charging system is it. Therefore, topologies with high frequencies and soft ng technique are used to reduce the charging current and extend battery life. Among these existing soft ng converters, class D resonant converters is the most r one because of its simplicity of circuit configuration, alization of the control scheme, low switching losses, gh flexibility for charging current regulation [21]-[22]. ass D resonant converters can be classified into three depending on the manner by which energy is extracted he resonant tank. These three types are the series it converter, parallel resonant converter, and series- converter.

terally, the series-resonant charger is formed by an r, a capacitor, and a bridge rectifier. The alternating (ac) through the resonant tank is rectified at the output ds, then, the output direct current (dc) charges the The series resonant converter seems to be suitable for tery charger applications but it shows a low voltage n with the switching frequency. Another shortcoming eries-resonant charger is that the current carried by the switches and resonant components is relatively loaded dently. The input impedance of the resonant topology low at the resonant frequency; this impedance equals to a of the parasitic resistances. As a result, a very high will flow through the resonant circuit and the switches, ; large conduction losses in the equivalent series ce and ripple voltage. In contrast to the series resonant er, the parallel-loaded resonant converter is able to the output voltage at no load by running at a frequency resonance. The parallel-loaded resonant converter s an inductive output filter and, thereby, the output through the capacitor is low, reducing the conduction nd the ripple voltage of the converter. Furthermore, the -loaded resonant converter is inherently short circuit d. Hence, the parallel-loaded resonant converter is itable for battery charger applications. Note also that ut voltage at resonance is a function of load and can ery high values at no load if the operating frequency is ed by the regulator. On the other hand, the series- converter combines the best characteristics of the esonant converters and parallel resonant converters. onant tank of this converter is the same as that of the -loaded resonant inverter, except for an additional r in series with the resonant inductor. The series- converter output can run over a wider input voltage d ranges from no-load to full load. For the series- converter with capacitive output filter, the analysis of er operation and the design of circuit parameters are c because the capacitive output stage is decoupled e resonant stage for a significant period during the ig cycle. Besides, the series-parallel converter cannot safely with a short circuit at switching frequency close to the resonant frequency. Therefore, the charging stage of the series-parallel converter has not been minimized and simplified, resulting in bulky size and high cost in the applications of battery chargers. Comparing the pre-mentioned three different class D resonant converter topologies, it appears that the parallel-loaded resonant converter is the best topology for battery charging applications because of its many merits. In addition, for battery charging applications, the parallel-loaded resonant converter is generally recommended as energy conversion stage due to its simple circuitry and typical input characteristics. The parallel-loaded resonant converter can be operated either below resonance or above resonance. The operation of parallel-loaded resonant converter below resonance has many disadvantages, such as use of RC snubbers and *dildt* limiting inductances needed for fast recovery diodes across the switches, etc. All these disadvantages can be overcome by operating the parallel-loaded resonant converter above resonance. Consequently, the work carried out here is for operation above resonance.

This paper is organized as follows. Section II summarizes the circuit description and operation principles of the proposed parallel-loaded resonant converter for battery charger. In Section III, the operating characteristics are introduced. Section IV shows the electronic implementation of the parallel-loaded resonant converter for battery charger. Finally, conclusions of this work are given in Section V.

II. CIRCUIT DESCRIPTION AND OPERATION PRINCIPLES

A. Circuit Description

Among the different charging topologies, the soft-switching scheme is the most attractive in recent years. Use of the soft-switching method has the advantages of reducing switching losses and extending the used life of the battery. In this paper, the proposed battery charger with parallel-loaded resonant converter is shown in Fig. 1. The two capacitors, C_1 and C_2, on the input are large and split the voltage of the input source. The elements L_r and C_r form the resonant tank. To facilitate the analysis, we assume that the power switching devices can be represented by a pair of bidirectional switches operated at a 50% duty ratio over a switching period T. For the half-bridge topology, each bidirectional power switch has an active power switch and an anti-parallel diode. The active power switches are driven by non-overlapping rectangular-wave trigger signals v_{GS1} and v_{GS2} with dead time. Thus, we may represent the effect of the power switches by means of an equivalent square-wave voltage source with an amplitude equal to $\pm V_s/2$. The resonant capacitor voltage is rectified to obtain a dc bus. The dc bus voltage can be varied and closely regulated by controlling the switching frequency. Because the ac-to-dc power conversion, in this case, is achieved by rectifying the voltage across capacitor C_r, a large filtering inductance L is needed to minimize the loading effect of the output circuit and to ensure that the current through it is mostly dc. Consequently, the current input to the bridge

I: (between $\omega_o t_0$ and $\omega_o t_2$)

e periodic switching of the resonant energy tank between $+V_S/2$ and $-V_S/2$ generates a square-wave across the input terminal. Since the output voltage is d to be a constant current I_O, the input current to the dge rectifier is $+I_O$ when v_{cr} is positive and is $-I_O$ when egative. Hence, Fig. 4 presents the equivalent circuit of half-bridge parallel-loaded resonant converter for the charger circuit in Fig. 2. This time interval ends when ches zero at $\omega_o t_2$.

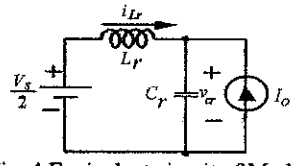

Fig. 4 Equivalent circuit of Mode I

fore $\omega_o t_0$, the active power switch S_2 is excited, and ts a current that equals the resonant tank current i_{Lr}. ive power switch S_1 is turned on at $\omega_o t_0$. However, the it tank current i_{Lr} is negative and flows through the eeling diode D_1. At the instant $\omega_o t_1$, the resonant tank i_{Lr} reverses and naturally commutates from eeling diode D_1 to the power switch S_1. In this mode, ver switches are turned on naturally at zero voltage and current. Accordingly, the active power switch is e after turn-on and positive before turn-off. The initial on of the capacitor C_r is V_{C0}. Then, the instantaneous it inductor current and the voltage across C_r can be ed, where the angular resonance frequency $\omega_o = \frac{1}{\sqrt{L_r C_r}}$ and the characteristic nce $Z_o = \sqrt{\frac{Lr}{Cr}}$, respectively.

$$= -I_O + (I_O + I_{L0})\cos\omega_o(t - t_0)$$

$$+ \left(\frac{\frac{V_S}{2} - V_{C0}}{Z_o}\right)\sin\omega_o(t - t_0) \qquad (1)$$

$$= \frac{V_S}{2} + \left(V_{C0} - \frac{V_S}{2}\right)\cos\omega_o(t - t_0)$$

$$- Z_o(I_O + I_{L0})\sin\omega_o(t - t_0) \qquad (2)$$

current in the switches is turned on at zero voltage and rrent to eliminate turn-on losses, but the switches are o turn off a finite current, so turn-off losses may exit. tely, small capacitors can be placed across the switches s snubbers to eliminate turn-off losses.

Mode II: (between $\omega_o t_2$ and $\omega_o t_3$)

This cycle starts at $\omega_o t2$ when capacitor voltage v_{cr} resonates from negative values to zero. At $\omega_o t_3$, before the half-cycle of the resonant current i_{Lr} oscillation ends, the switch S_1 is forced to turn off, forcing the positive current to flow through the bottom freewheeling diode D_2. Figure 5 displays the equivalent circuit.

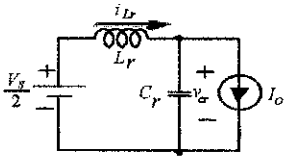

Fig. 5 Equivalent circuit of Mode II

The positive dc input voltage applied across the resonant tank causes the resonant current that flows through the power switch to go quickly to zero at $\omega_o t_2$. During this interval, the inductor current i_{Lr} is expressed as follows, where I_{L1} is the initial current in the inductor i_{Lr}.

$$i_{Lr}(t) = I_O + (I_{L1} - I_O)\cos\omega_o(t - t_3) + \left(\frac{\frac{V_S}{2} - V_{c1}}{Z_o}\right)\sin\omega_o(t - t_3) \qquad (3)$$

$$I_{L1} = i_{Lr}(t = t_2) = -I_O + (I_O + I_{L0})\cos\alpha + \left(\frac{\frac{V_S}{2} - V_{c0}}{Z_o}\right)\sin\alpha$$

The voltage v_{cr} across the resonant capacitor C_r is given by Eq. (4), where V_{c1} is the initial voltage across the capacitor C_r.

$$v_{Cr}(t) = \frac{V_S}{2} + \left(V_{C1} - \frac{V_S}{2}\right)\cos\omega_o(t - t_3) + Z_o(I_{L1} - I_O)\sin\omega_o(t - t_3) \qquad (4)$$

$$V_{c1} = v_{cr}(t = t_2) = \frac{V_S}{2} + \left(V_{c0} - \frac{V_S}{2}\right)\cos\alpha + Z_o(I_O + I_{L0})\sin\alpha$$

Mode III: (between $\omega_o t_3$ and $\omega_o t_5$)

A turn-off trigger signal is applied to the gate of the active power switch S_1. Then, the inductor current naturally commutates from the active power switch S_1 to the freewheeling diode D_2.

Mode III begins at $\omega_o t_3$, when the diode D_2 is turned on as displayed in Fig. 6, producing a resonant stage between inductor L_r and capacitor C_r. The inductor L_r and capacitor C_r resonate. Then, the inductor current i_{Lr} and the capacitor voltage v_{cr} of the resonant circuit are given as Eq.(5) and Eq.(6), where V_{c2} is the initial voltage across the resonant

r has constant amplitudes $+I_O$ and - I_O, depending on
r the voltage $v_{Cr}(t)$ is positive or negative, respectively.
equency of this current waveform is the same as that of
tching frequency. With these observations, the parallel-
nt converter can be modeled as a series LC circuit and a
-wave current source $\pm I_O$ in parallel with the resonant
or. The simplified equivalent circuit for the battery
r with parallel-loaded resonant converter is given in Fig.

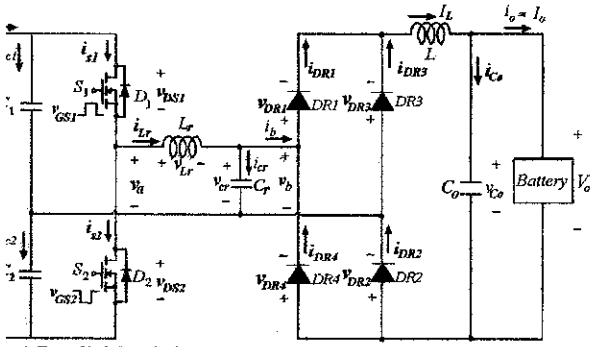

g.1 Parallel-loaded resonant converter for battery charger

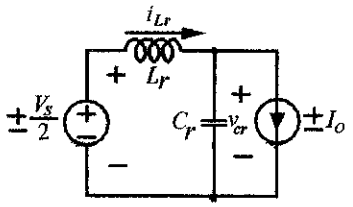

2 Simplified equivalent circuit of parallel-loaded resonant converter for battery charger

uit Operation Principles

ure 3 displays the idealized steady-state voltage and
waveforms in the class-D half-bridge parallel-loaded
nt converter for a switching frequency f_S that exceeds
onant frequency f_O. Operation above resonance is
ed because the power switches turn on at zero current
o voltage; thus, the freewheeling diodes do not need to
ery fast reverse-recovery characteristics. During the
e half-cycle of the voltage across the resonant capacitor,
wer is supplied to the battery through diodes D_{r1} and
uring the negative half-cycle of the voltage across the
nt capacitor, the power is fed to the battery through
D_{r3} and D_{r4}.

s-D half-bridge parallel-loaded resonant converter for
charger is analyzed based on the following
tions:

Switching elements of the converter are ideal, such that the decline in forward voltage in the on-state resistance of the switch is negligible.

The equivalent series resistance of the capacitance and stray capacitances is negligible.

3) The characteristics of passive components are assumed to be linear, time-invariant and frequency-independent.
4) The filter inductor L at the output terminal of the full-bridge rectifier is usually very large, and therefore the output current through the inductor L can be treated as a dc current in each switching cycle.
5) Active power switches S_1 and S_2 are on and off alternately, applying a square-wave voltage across the parallel-resonant circuit. If the load quality factor of the class-D half-bridge parallel-loaded resonant converter is sufficiently high, the resonant current, i_{Lr}, is sinusoidal.

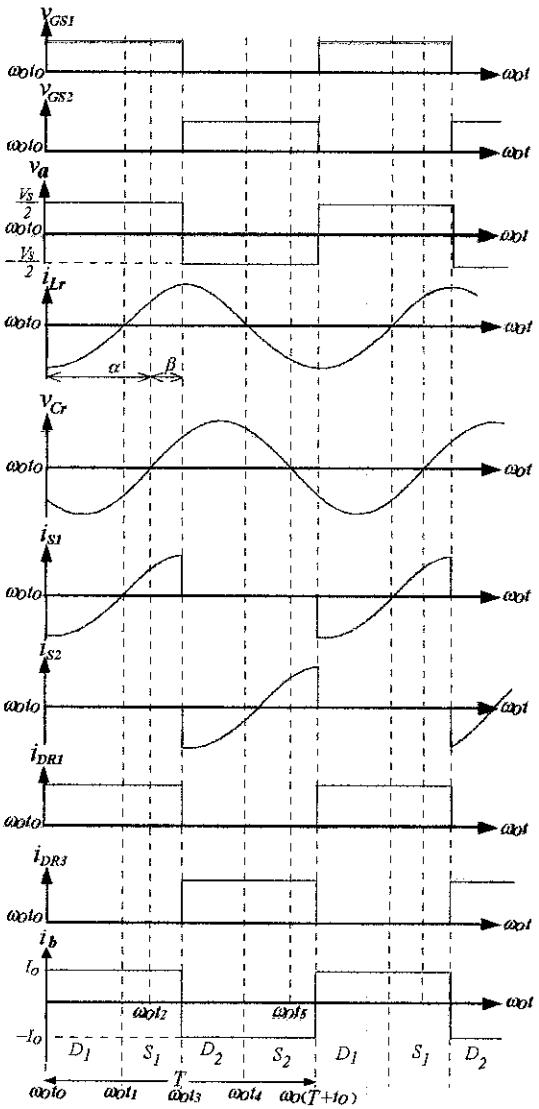

Fig. 3 Idealized voltage and current waveforms

The steady-state operation of the parallel-load resonant charging circuit in one switching period can be divided into four modes.

or C_r and $I_{L2}$is the initial current of the resonant
r, respectively.

$$= I_O + (I_{L2} - I_O)\cos\omega_O(t - t_3) + \left(\frac{\frac{V_S}{2} + V_{c2}}{Z_O}\right)\sin\omega_O(t - t_3) \quad (5)$$

$$= -\frac{V_S}{2} + \left(\frac{V_S}{2} + V_{c2}\right)\cos\omega_O(t - t_3) + Z_O(I_{L2} - I_O)\sin\omega_O(t - t_3) \quad (6)$$

$$i_{Lr}(t = t_2) = I_O + (I_{L1} - I_O)\cos\beta + \left(\frac{\frac{V_S}{2} - V_{c1}}{Z_O}\right)\sin\beta$$

$$v_{cr}(t = t_2) = \frac{V_S}{2} + \left(V_{c1} - \frac{V_S}{2}\right)\cos\beta + Z_O(I_{L1} - I_O)\sin\beta$$

fore $\omega_o t_4$, the trigger signal v_{gs2} excites the active power S_2. When the capacitor voltage v_{Cr} changes direction, ifier diodes D_{r1} and D_{r2} are turned off at the instant $\omega_o t_5$ de III ends. Figure 6 shows the equivalent circuit.

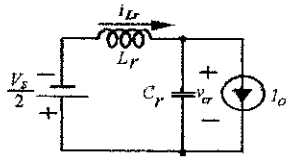

Fig. 6 Equivalent circuit of Mode III

IV: (between $\omega_o t_5$ and $\omega_o t_6$)

hen the capacitor voltage v_{Cr} is negative, the rectifier D_{r3} and D_{r4} are turned on with zero-voltage condition at ant $\omega_o t_5$. Figure 7 depicts the equivalent circuit.

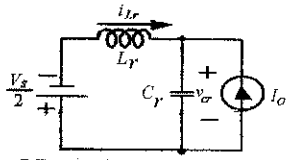

Fig. 7 Equivalent circuit of Mode IV

plying Kirchhoff's law to Fig. 7 yields the inductor i_{Lr} as Eq.(7)

$$= -I_O + (I_O + I_{L3})\cos\omega_O(t - t_5) - \left(\frac{\frac{V_S}{2} + V_{c3}}{Z_O}\right)\sin\omega_O(t - t_5) \quad (7)$$

uation (8) gives the voltage v_{cr} of the resonant or.

$$v_{cr}(t) = -\frac{V_S}{2} + \left(\frac{V_S}{2} + V_{c3}\right)\cos\omega_O(t - t_5) + Z_O(I_O + I_{L3})\sin\omega_O(t - t_5) \quad (8)$$

Then, the initial inductor current of this mode can be written as follows.

$$I_{L3} = i_{Lr}(t = t_5) = I_O + (I_{L2} - I_O)\cos\omega_O(t_5 - t_3) - \left(\frac{\frac{V_S}{2} + V_{c2}}{Z_O}\right)\sin\omega_O(t_5 - t_3)$$

The following equation yields the initial value V_{c3} in the previous mode, to yield the following equation.

$$V_{c3} = v_{cr}(t = t_5) = -\frac{V_S}{2} + \left(\frac{V_S}{2} + V_{c2}\right)\cos\omega_O(t_5 - t_3) + Z_O(I_{L2} - I_O)\sin\omega_O(t_5 - t_3)$$

The inductor current and the capacitor voltage at $t=t_6$ can be calculated as follows.

$$I_{L4} = i_{Lr}(t = t_6) = -I_O + (I_O + I_{L3})\cos\omega_O(t_6 - t_5) - \left(\frac{\frac{V_S}{2} + V_{c3}}{Z_O}\right)\sin\omega_O(t_6 - t_5)$$

$$V_{c4} = v_{cr}(t = t_6) = -\frac{V_S}{2} + \left(\frac{V_S}{2} + V_{c3}\right)\cos\omega_O(t_6 - t_5) + Z_O(I_O + I_{L3})\sin\omega_O(t_6 - t_5)$$

When the driving signal V_{gs1} again excites the active power switch S_1, this mode ends and the operation returns to mode I in the subsequent cycle.

During the positive half-cycle of the capacitor voltage, the power is supplied to the battery through the output rectifier diodes D_{R1} and D_{R2}. During the negative half-cycle of the inductor current, the power is supplied to the battery through the output rectifier diodes D_{R3} and D_{R4}.

III. OPERATING CHARACTERISTICS

Figure 8 presents the rectifier stage of the class-D half-bridge parallel-loaded resonant converter for battery charger. The switching frequency of the active power switches is assumed to exceed the resonant frequency such that the resonant current is continuous. Given a large inductor filter at the output terminal, the charging current may be assumed to be constant.

The charger circuit in Fig. 2 can be simplified to the schematic circuit shown in Fig. 8 to facilitate the analysis of the operation of the class-D half-bridge parallel-loaded resonant converter. In the full-bridge rectifier, when v_{cr} is positive, diodes D_{R1} and D_{R2} conduct and $v_{bO}=v_b$ and $i_O=I_O$. When v_{cr} goes negative, diodes D_{R3} and D_{R4} conduct,

re, $v_{bO}=v_b$ and $i_O=-I_O$. Accordingly, at any time, the output voltage of the full-bridge rectifier can be ;ed as

$$v_b|$$

$$v_{b1m}\sin\omega t| \quad (9)$$

ıce the output current is assumed to be a constant I_o, e input current to the output full-bridge rectifier, v_b, is en v_{Cr} is positive and is $-I_o/2$ when v_{Cr} is negative.

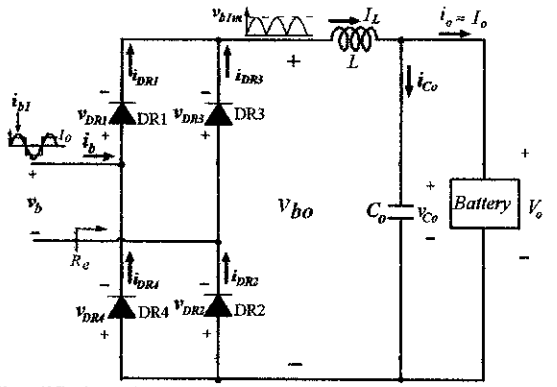

ilmplified equivalent output stage of the class-D half-bridge arallel-loaded resonant converter for battery charger

e class-D half-bridge parallel-loaded resonant er for battery charger is analyzed based on the ental frequency of the Fourier series of the voltages rrents. Then, the output voltage v_b of the full-bridge r can be obtained by assigning an arbitrary time origin Fig. 8 and then integrating $v_b(t)=v_{b1m}\sin\omega t$ over one-iod.

$$:\int_0^{\pi} V_{b1m}\sin\omega t\, d(\omega t)$$

$$\frac{V_{b1m}}{\pi} \quad (10)$$

uation (11) gives the amplitude of the voltage v_b and g voltage v_O

$$:\frac{\pi}{2}\cdot V_O \quad (11)$$

e ac-side current of the full-bridge rectifier can be ed as

$$\begin{cases} +I_O & if \quad v_{cr}>0 \\ -I_O & if \quad v_{cr}<0 \end{cases} \quad (12)$$

transition between the two values is instantaneous due ssumption of large filter inductor L.

e error due to this approximation is very small when tching frequency is higher than the resonant frequency. ;ase of the square-wave current i_b, the Fourier series s the odd harmonics and can be represented as Eq.

$$i_b(t)=\sum_{n=1,3,5....}^{\infty}\frac{4I_O}{n\pi}\sin(n\omega t) \quad (13)$$

Equation (14) gives the peak value of the fundamental component of current i_b.

$$i_{b1}=\frac{4I_O}{\pi}\sin(\omega t) \quad (14)$$

The output resistance in this equivalent circuit of the parallel-loaded resonant converter is determined from the ratio of voltage to current at the input terminal of the full-bridge rectifier. Equation (15) thus defines resistance.

$$R_e=\frac{V_{b1m}}{I_{b1}}=\frac{\pi^2}{8}\cdot\frac{V_O}{I_O} \quad (15)$$

The relationship between input and output is approximated by ac circuit analysis using the fundamental frequencies of the voltage and current equations. Figure 9 plots the equivalent ac circuit.

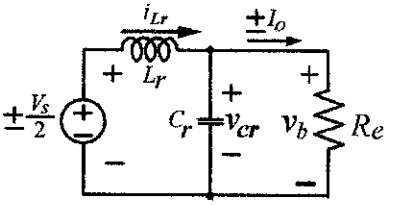

Fig.9 Equivalent ac circuit of class-D half-bridge parallel-loaded resonant converter for battery charger

To achieve resonant operation, the resonant circuit must be underdamped. That is

$$R_e \geq 2\sqrt{\frac{L_r}{C_r}} \quad (13)$$

The input part of the class-D half-bridge parallel-loaded resonant converter for battery charger has a dc input voltage source V_S and a set of bidirectional power switches. The active power switches are controlled to generate a square-wave voltage v_a. Since a resonant circuit forces a sinusoidal current, only the power of the fundamental component is transferred form the input source to the resonant circuit. Therefore, only the fundamental component of this converter need be considered. Equation (14) defines a voltage transfer function of the parallel-loaded resonant converter.

$$\frac{V_O}{V_s}=\frac{4}{\pi^2\sqrt{\left(1-\frac{X_L}{X_C}\right)^2+\left(\frac{X_L}{R_e}\right)^2}} \quad (14)$$

The reactance X_L and X_C depend on the switching frequency. Accordingly, the output voltage can be regulated by changing the switching frequency of the converter. The normalized output voltage V_o/V_s is plotted as a function of f_s/f_o

ous loaded quality factors Q. This figure indicates that lf-bridge parallel-loaded resonant converter output can be larger than the input voltage [21]. Therefore, nverter is quite appropriate for use in situations that low input voltage and high output current, especially ddle power levels (as in this application, charging s), due to its simple circuitry and typical input eristics.

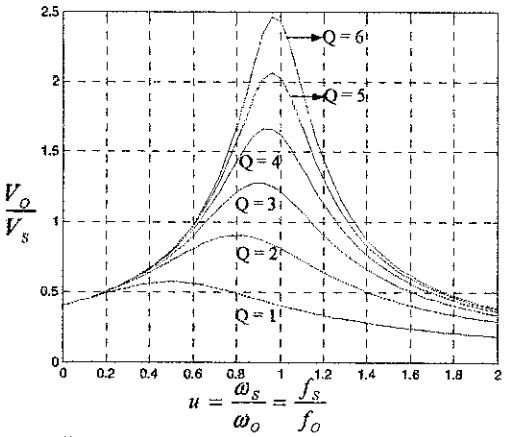

Normalized output voltage at various switching frequencies

e energy that flows into the battery during the interval $\omega_o t \leqq \omega_o t_2$ is given by Eq. (15).

$$\int_0^{t_2-t_0} -I_O v_{cr}(t)dt$$

$$\frac{I_O}{\omega_O}\left[\frac{V_S}{2}\alpha+\left(V_{C0}-\frac{V_S}{2}\right)\sin\alpha+Z_O(I_O+I_{L0})(1-\cos\alpha)\right]$$

$$\frac{I_O}{\omega_O}A \qquad (15)$$

e following term is defined.

$$-\alpha+\left(V_{C0}-\frac{V_S}{2}\right)\sin\alpha+Z_O(I_O+I_{L0})(1-\cos\alpha)\Big] \quad (16)$$

e energy that flows into the battery during the interval $\omega_o t \leqq \omega_o t_3$ is given by Eq. (17).

$$\int_0^{t_3-t_2} I_O v_{cr}(t)dt$$

$$\frac{I_O}{\omega_O}\left[\frac{V_S}{2}\beta+\left(V_{C1}-\frac{V_S}{2}\right)\sin\beta+Z_O(I_{L1}-I_O)(1-\cos\beta)\right] \quad (17)$$

bstituting Eqs. (3) and (4) into the above equation Eq.(18).

$$\frac{2}{\omega_O}\left\{\frac{V_S}{2}\beta+\left[\left(V_{CO}-\frac{V_S}{2}\right)\cos\alpha+Z_O(I_O+I_{LO})\sin\alpha\right]\sin\beta\right.$$

$$\left.I_O+(I_O+I_{LO})\cos\alpha\right]+\left(\frac{\frac{V_S}{2}-V_{CO}}{Z_O}\right)\sin\alpha](i-\cos\beta)\}(18)$$

which can be rewritten as

$$\varepsilon_{L2}=\frac{I_O}{\omega_O}\{\frac{V_S}{2}\beta+2Z_OI_O(\cos\beta-1)+(\frac{V_S}{2}-V_{CO})[\sin\alpha-\sin(\alpha+\beta)]$$

$$+Z_O(I_O+I_{LO})[\cos\alpha-\cos(\alpha+\beta)]\} \qquad (19)$$

The following term is defined.

$$B\equiv\{\frac{V_S}{2}\beta+2Z_OI_O(\cos\beta-1)+(\frac{V_S}{2}-V_{CO})[\sin\alpha-\sin(\alpha+\beta)]$$

$$+Z_O(I_O+I_{LO})[\cos\alpha-\cos(\alpha+\beta)]\} \qquad (20)$$

Hence, the total energy that flows into the battery during the interval $\omega_o t_0 \leqq \omega_o t \leqq \omega_o t_2$ is determined by Eq. (21).

$$\varepsilon_L=\varepsilon_{L1}+\varepsilon_{L2}=\frac{I_O}{\omega_O}(B-A) \qquad (21)$$

The energy from the input dc source during the interval $\omega_o t_0 \leqq \omega_o t \leqq \omega_o t_2$ is given by Eq. (22).

$$\varepsilon_{S1}=\frac{V_S}{2}\int_0^{t_2-t_0} i_{Lr}(t)dt$$

$$=\frac{V_S}{2\omega_O}\left[-I_O\alpha+(I_O+I_{LO})\sin\alpha+\left(\frac{V_S-V_{C0}}{Z_O}\right)(1-\cos\alpha)\right] \qquad (22)$$

The following term is defined.

$$C\equiv\left[-I_O\alpha+(I_O+I_{LO})\sin\alpha+\left(\frac{V_S-V_{C0}}{Z_O}\right)(1-\cos\alpha)\right] \qquad (23)$$

The energy from the input dc source during the interval $\omega_o t_2 \leqq \omega_o t \leqq \omega_o t_3$ is given by Eq. (24).

$$\varepsilon_{S2}=\frac{V_S}{2}\int_0^{t_3-t_2} i_{Lr}(t)\cdot dt$$

$$=\frac{V_S}{2\omega}\{I_O\beta+[-2I_O+(I_O+I_{LO})\cos\alpha+(\frac{\frac{V_S}{2}-V_{CO}}{Z_O})\sin\alpha]\sin\beta$$

$$+[(\frac{\frac{V_S}{2}-V_{CO}}{Z_O})\cos\alpha-(I_O+I_{LO})\sin\alpha](1-\cos\beta)\} \qquad (24)$$

The following term is defined.

$$D\equiv\{I_O(\beta-2\sin\beta)+(I_O+I_{LO})[\sin(\alpha+\beta)-\sin\alpha]$$

$$+(\frac{\frac{V_S}{2}-V_{CO}}{Z_O})[\cos\alpha-\cos(\alpha+\beta)]\} \qquad (25)$$

Accordingly, the energy that is generated by the input dc source is given by Eq. (26).

$$W_S=W_{S1}+W_{S2}=\frac{V_S}{2\omega_O}(C+D) \qquad (26)$$

For a lossless system, these two energies are equal in the steady state. Therefore, Eq.(27) gives the output voltage.

$$V_O=\frac{V_S}{2}\frac{C+D}{B-A} \qquad (27)$$

The ac sinusoidal wave on the load side of the charger filtered by the resonant tank is rectified by the full-bridge rectifier, which is then regulated by the L-C low-pass filter at

put terminal. The regulated voltage and current charge tery after they are filtered. The ripple following high- ıcy filtering is smaller than that at low-frequency. a voltage and current more like pure dc are more useful rging a battery. The parallel-load resonant charger is a g device with a constant current as determined by the nt of filtering type at output terminal. The most ınt advantage of the parallel-loaded resonant converter the maximum charging efficiency for the proposed er operating above resonance can be obtained. This ıge makes the parallel-loaded resonant converter ed configuration for battery charger applications.

IV. EXPERIMENT RESULTS

e input of the proposed parallel-loaded resonant er was connected to a system that comprised a dc with an output voltage of 30V. A prototype of the charger with parallel-loaded resonant topology was hed in a laboratory to verify the functional operations. veloped charger circuit is applied to a 12V, 48Ah lead- attery. The conditions of the experiment were as : switching frequency f_S=82 kHz, resonant frequency Hz, charging current I_o = 6.5A, charging voltage V_{BA} = and the open circuit voltage of battery V_{OC} = 11V. these operating conditions, the two parameters of the -loaded resonant converter are as follows.

=1 μF

4 μH

waveforms were measured using a digital multi-meter. 11 plots the waveforms of the trigger signals V_{GS1}, and igure 12 displays the voltage and current waveforms of ve power switch S_1. Figure 13 depicts the voltage and waveforms of the input terminal of resonant tank. Fig. ches the voltage waveform of resonant capacitor v_{Cr} current waveform of resonant inductor i_{Lr}.

ıre 15 shows the input voltage and output voltage rms of the resonant tank terminals. Figure 16 illustrates put voltage waveform of the resonant tank terminals input current waveform of the full-bridge rectifier. 17 displays the voltage and current waveforms of the r diodes D_{R1} and D_{R2}. Figure 18 shows the charging and current waveforms of battery terminal. From this we can see that the output is a smooth dc voltage and , which is the ideal circuit for a battery charger. Figure icts the voltage variation curve of the battery. The l voltage of the battery rises from 10.5V to 15.5V in nutes. Figures 20 and 21 plot the charging current and rging efficiency, respectively. The charging current 00 minutes to maintain around 6.4A. The minimal and l efficiencies of the battery charging circuit are about and 90.9%, respectively, and the average charging cy of the battery charger is 88.8%.

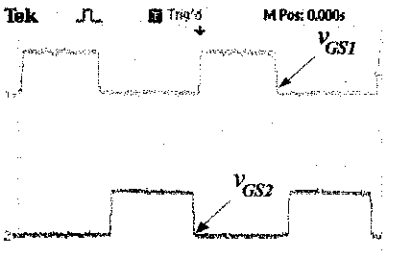

CH1:10V/div CH2:10V /div Time:2.5μs /div

Fig. 11 Trigger signals of power switches

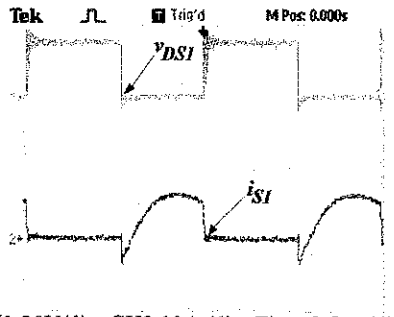

CH1:20V/div CH2:10A /div Time:2.5μs /div

Fig. 12 Voltage and current waveforms of active power switch S_1

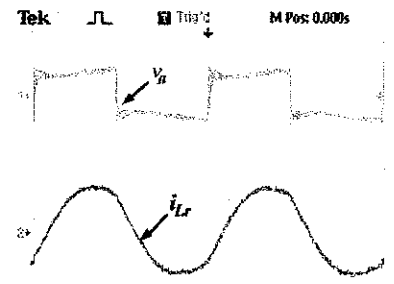

CH1:20V/div CH2:10A /div Time:2.5μs /div

Fig. 13 Voltage and current waveforms of the input terminal of resonant tank

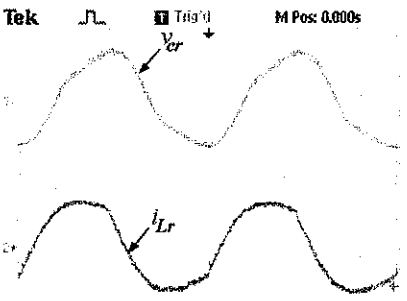

CH1:20V/div CH2:10A /div Time:2.5μs /div

Fig. 14 Voltage waveform of resonant capacitor and current waveform of resonant inductor

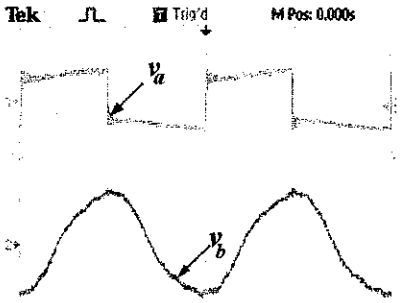

CH1:20V/div CH2: 20V /div Time:2.5μs /div
. 15 Input and output voltage waveforms of resonant tank

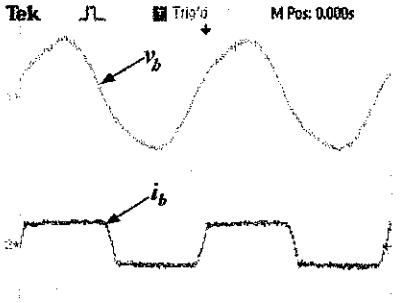

CH1:20V/div CH2: 10V /div Time:2.5μs /div
ure 16 The output voltage waveform of the resonant tank terminals and the input current waveform of the full-bridge rectifier

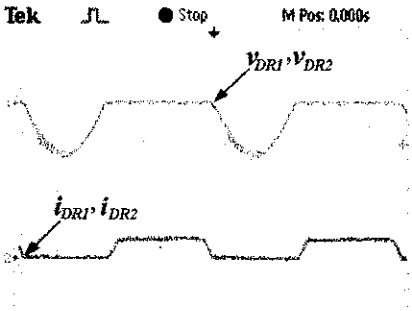

CH1:20V/div CH2:10A /div Time:2.5μs /div
Voltage and current waveforms of rectifier diodes D_{R1} and D_{R2}

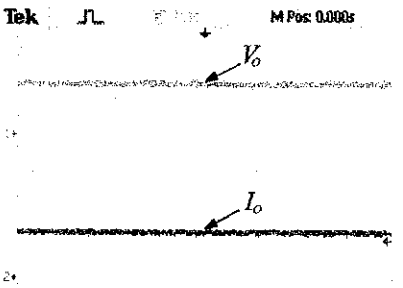

CH1:10V/div CH2:5A /div Time:2.5μs /div
Charging voltage and current waveforms of battery terminal

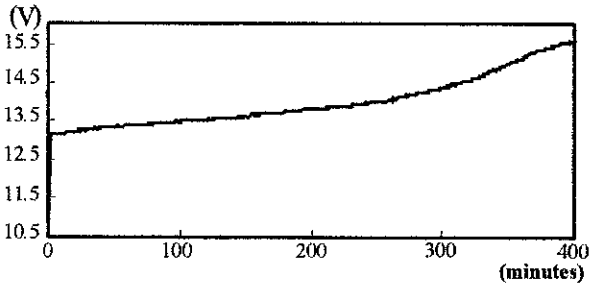

Fig. 19 Battery voltage during charging period

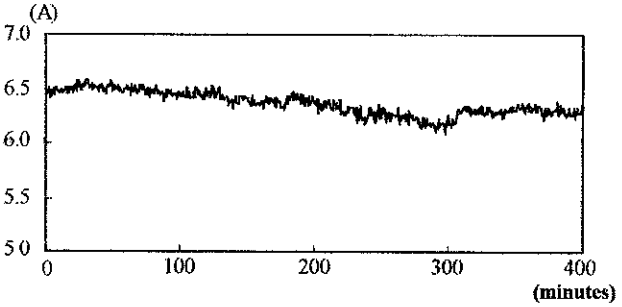

Fig. 20 Charging current during charging period

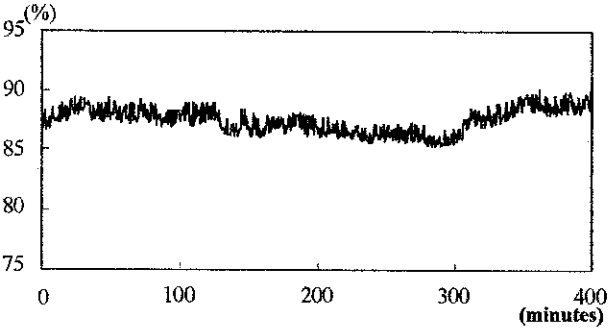

Fig. 21 Charging efficiency during charging period

V. Conclusions

This work designed a parallel-loaded resonant converter with full-bridge rectifier for battery charger. The circuit structure is simpler and cheaper than other control mechanisms which require many components. The developed charger offers the advantages of zero-voltage switching, reduced switching losses, and increased charging efficiency. The charging current can be determined from the characteristic impedance of the resonant tank by the adjustable switching frequency of the converter, whereas the parallel-load resonant converter is applied to battery charger to yield the required charging conditions. The experimental results demonstrate the effectiveness of the developed charger. The maximum charging efficiency is 90. 9%, which is quite satisfactory when the high-frequency parallel-loaded resonant circuit is applied to a battery charger. Compared with conventional battery chargers, charging efficiency can be improved using the parallel-loaded resonant converter with full-bridge rectifier topology. Favorable performance is obtained at lower cost and with fewer circuit components.

REFERENCES

Wongsaichua, W. J. Lee, S. Oraintara, C. Kwan, F. Zhang, egrated High-Speed Intelligent Utility Tie Unit for bursed/Renewable Generation Facilities," IEEE Transactions on ustry Applications, Vol. 41, No. 2, March/April 2005, pp. 507-513.

ipley, M. T. Ansari,J. Dehn, "Battery Chargers and Batteries for DC AC Back-up Power Systems," IEEE Industry Applications Society n Annual Petroleum and Chemical Industry Conference, September l, pp.139-144.

ng Du, Burak Ozpineci, Leon M. Tolbert, and John N. Chiasson, C–AC Cascaded H-Bridge Multilevel Boost Inverter with No uctors for Electric/Hybrid Electric Vehicle Applications," IEEE nsactions on Industry Applications, Vol. 45, No. 3, May/June 2009, 963-970.

Schuch, C. Rech, H. L. Hey, H. A. Grundling, H. Pinheiro, J. R. heiro, "Analysis and Design of a New High-Efficiency Bidirectional grated ZVT PWM Converter for DC-Bus and Battery-Bank rface," IEEE Transactions on Industry Applications, Vol. 42, No. 5, tember/October 2006, pp. 1321-1332.

J. Zhou, X. Zhang, P. Xu, and W. X. Shen, "Single-Phase nterruptible Power Supply Based on Z-Source Inverter," IEEE nsactions on Industry Electronicss, Vol. 55, No. 8, August 2008, pp. 7-3004.

M. Lukic, J. Cao, R. C. Bansal, F. Rodriguez, and A. Emadi, "Energy rage Systems for Automotive Applications," IEEE Transactions on ustry Electronicss, Vol. 55, No. 6, June 2008, pp. 2258-2267.

Dondi, A. Bertacchini, D. Brunelli, L. Larcher, and L. Benini, odeling and Optimization of a Solar Energy Harvester System for -Powered Wireless Sensor Networks," IEEE Transactions on ustry Electronics, Vol. 55, No. 7, July 2008, pp. 2759-2766.

Ceraolo, "New Dynamical Models of Lead-Acid Batteries," IEEE nsactions on Power Systems, Vol. 15, No. 4, November 2000, pp. 4-1190.

Kutluay, Y. Çadırcı, Y. S. Özkazanç,. and I. Çadırcı, "A new online e-of-charge estimation and monitoring system for sealed lead-acid eries in Telecommunication power supplies," IEEE Transactions on ustry Electronicss, Vol. 52, No. 5, October 2005, pp. 1315-1327.

P. Jenkins, J. Fletcher, and D. Kane, "Lifetime Prediction and Sizing Lead-Acid Batteries for Microgeneration Storage Applications," IET- newable Power Generation, Vol. 2, No.3, September 2008, pp. 191- .

J. Chiu, L. W. Lin, P. L. Pan, and M. H. Tseng ,"A Novel Rapid rger for Lead-Acid Batteries with Energy Recovery," IEEE nsactions on Power Electronics, Vol. 21, No. 3, May 2006, pp. 640- .

M. Morcos, N. G. Dillman, C. R. Mersman, "Battery chargers for tric vehicles," IEEE Transactions on Engingeering Review, Vol. 20, 11, November 2000, pp. 8-11.

Chen, and G. A. Rincón-Mora ,"Accurate, Compact, and Power- cient Li-Ion Battery Charger Circuit," IEEE Transactions on Circuit Systems II: Express Briefs, Vol. 53, No. 11, September 2006, pp. 0-1184.

S. Hwang, S. C. Wang, F. C. Yang, and J. J. Chen, "New Compact OS Li-Ion Battery Charger Using Charge-Pump Technique for table Applications," IEEE Transactions on Circuit and Systems I: ular Papers, Vol. 54, No. 14, April 2007, pp. 705-712.

C. Chuang, Y. L. Ke, H. S. Chuang, H. K. Chen, "Implementation Analysis of an Improved Series-Loaded Resonant DC–DC verter Operating Above Resonance for Battery," IEEE Transactions industry Applications, Vol. 45, No. 3, May/June 2009, pp. 1052-1059.

Jiang, and R. A. Dougal, "Control Strategies for Active Power ring in a Fuel-Cell-Powered Battery-Charging Station," IEEE nsactions on Industry Applications, Vol. 40, No. 3, May/June 2004, 917-924.

Chunlei , B. C. Walker, E. Zeisel, B. Hu, G. H. McAllister, "A Highly grated Power Management IC for Advanced Mobile Applications," IEEE Journal of Solid-State Circuits, Vol. 42, No. 8, August 2007, pp. 1723-1731.

[18] Y. C. Chuang, and Y. L. Ke, "High-Efficiency and Low-Stress ZVT–PWM DC-to-DC Converter for Battery Charger," IEEE Transactions on Industry Electronicss, Vol. 55, No. 8, August 2008, pp. 3030-3037.

[19] L. R. Chen, J. J. Chen, N. Y. Chu, and G. Y. Han, "Current-Pumped Battery Charger," IEEE Transactions on Industry Electronicss, Vol. 55, No. 6, June 2008, pp. 2482-2488.

[20] Y. C. Chuang, and Y. L. Ke, "High Efficiency Battery Charger with a Buck Zero-Current-Switching Pulse-Width-Modulated Converter," IET Power Electronics, Vol. 1, No. 4, December 2008, pp. 433-444.

[21] M. K. Kazimierczuk and D. Czarkowski, "Resonant Power Converters," Wiley, New York, 1995.

[22] H. Abe, H. Sakamoto, and K. Harada, "A Noncontact Charger Using a Resonant Converter with Parallel Capacitor of the Secondary Coil," IEEE Transactions on Industry Applications, Vol. 36, No. 2, March/April 2000, pp. 444-451.

APPLICATION NOTE

RESONANT CONVERTER TOPOLOGIES

by M. Bildgen

1. INTRODUCTION

Increasing the frequency of operation of power converters is desirable, as it allows the size of circuit magnetics and capacitors to be reduced, leading to cheaper and more compact circuits. However, increasing the frequency of operation also increases switching losses and hence reduces system efficiency. One solution to this problem is to replace the "chopper" switch of a standard SMPS topology (Buck, Boost etc.) with a "resonant" switch, which uses the resonances of circuit capacitances and inductances to shape the waveform of either the current or the voltage across the switching element, such that when switching takes place, there is no current through or voltage across it, and hence no power dissipation - see figure 1. A circuit employing this technique is known as a resonant converter (or, more accurately, a quasi-resonant converter, as only part of the resonant sinusoid is utilized).

A Zero Current Switching (ZCS) circuit shapes the current waveform, while a Zero Voltage Switching (ZVS) circuit shapes the voltage waveform.

2. ZERO CURRENT SWITCH

A typical Zero Current Switch consists of a switch, S, in series with the resonant inductor L_{RES}, and the resonant capacitor C_{RES} connected in parallel. Energy is supplied by a current source.The circuit and waveforms are shown in figure 2.

If an output transformer is used, in certain cases its parasitic inductance can be used as the resonant inductance (in both this and the zero voltage topology). However, as its value is generally not known, the resonant frequency will not be fixed, which may cause problems in the circuit design.

When the switch S is off, the resonant capcitor is charged up with a more or less constant current, and so the voltage across it rises linearly.

When the switch is turned on, the energy stored in the capacitor is transferred to the inductor, causing a sinusoidal current to flow in the switch. During the negative half wave, the current flows through the anti-paralleled diode, and so in this period there is no current through or voltage across the switch; and it can be turned off without losses.

This type of switching is also known as thyristor mode, as it is one of the more suitable ways of using thyristors; these devices will only turn off if the current through them is forced to zero, which occurs naturally in this topology.

Figure 1. Current and voltage waveforms of hard and resonant switching systems

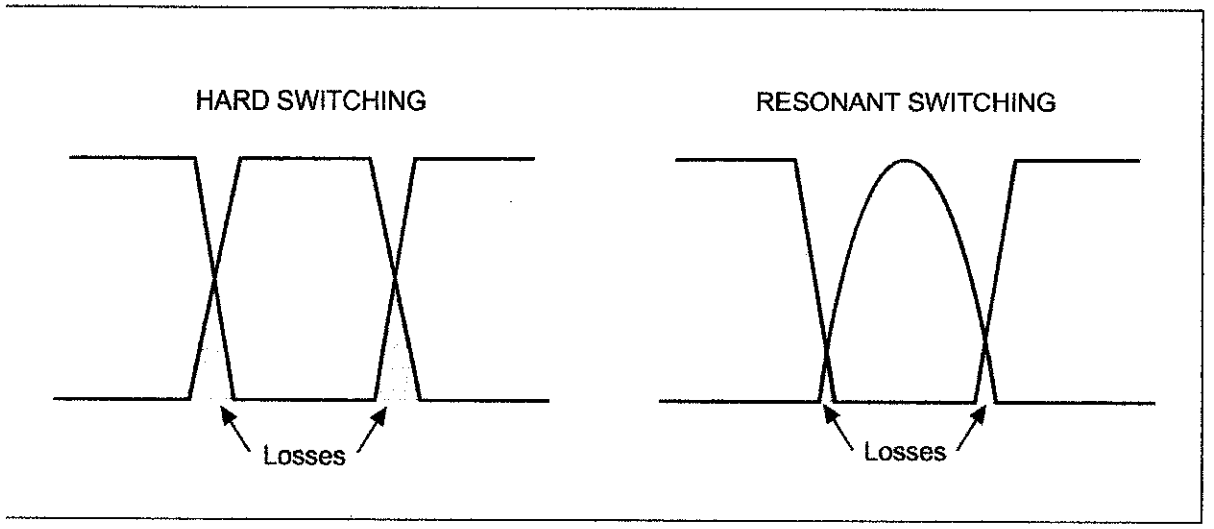

3. ZERO VOLTAGE SWITCH

A typical Zero Voltage Switch consists of a switch in series with a diode. The resonant capacitor is connected in parallel, and the resonant inductor is connected in series with this configuration. A voltage source connected in parallel injects the energy into this system. The circuit and waveforms are shown in figure 3.

When the switch is turned on, a linear current flows through the inductor. When the switch turns off, the energy that is stored in the inductor flows into the resonant capacitor. The resulting voltage across the capacitor and the switch is sinusoidal. The negative half-wave of the voltage is blocked by the diode. During this negative half wave, the current and voltage in the switch are zero, and so it can be turned on without losses.

4. POWER SEMICONDUCTORS IN RESONANT CONVERTERS

Because they require a substantial drive current, Bipolar transistors are not generally used in resonant converters, unless the base drive is provided by the resonant circuit itself (for example in TV deflection circuits and fluorescent lamp ballasts). Power MOSFETs and IGBTs, with their effectively capacitive inputs and low drive energy requirements, are the most frequently used types.

The graph in figure 4 shows the die size of Power MOSFETs and IGBTs required to conduct 1 amp with a voltage drop of 2 volts, against the maximum rated voltage. For low voltage applications, the MOSFET is interesting, as the die size is very small (and so the device is cheap). However for higher breakdown voltages, the IGBT is more suitable, as

Figure 2. Full-wave zero-current switch - topology and waveforms

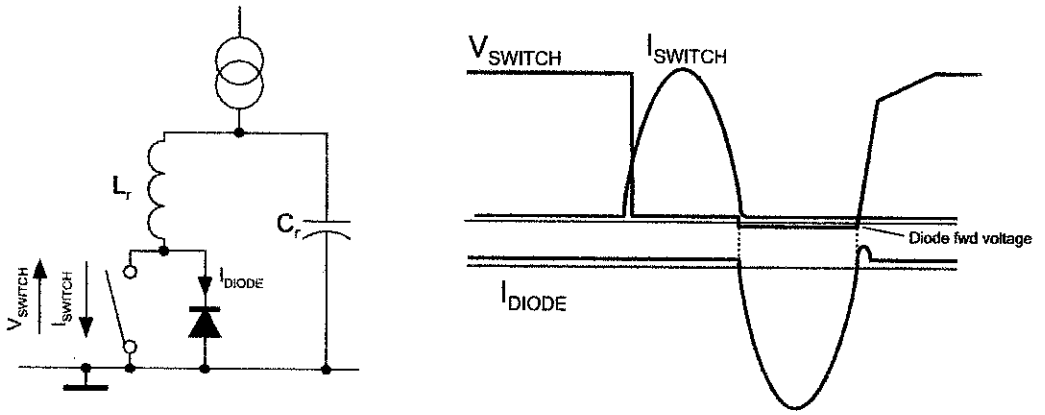

Figure 3. Full-wave zero-voltage switch - topology and waveforms

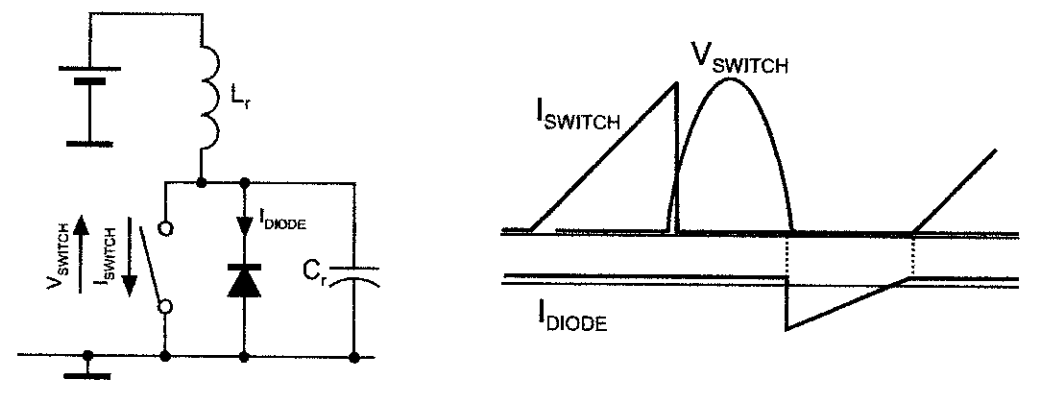

Figure 4. Comparison of MOSFET and IGBT

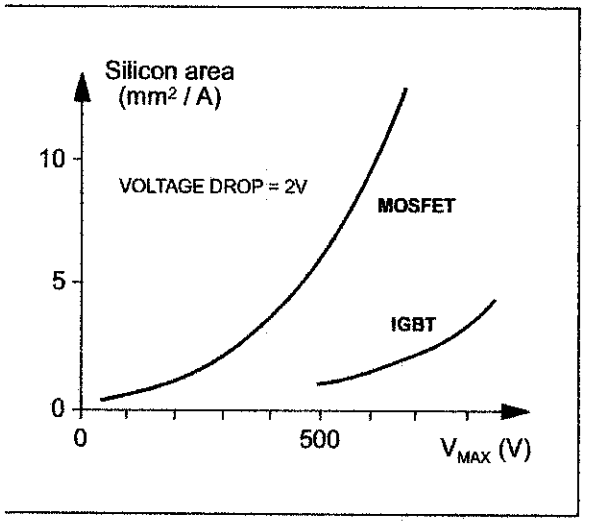

Figure 5. Simple MOSFET model

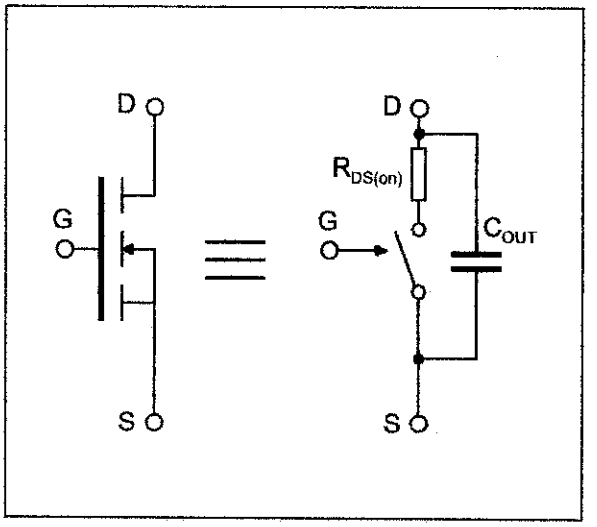

he die size required is almost constant approaching he maximum rated voltage.

4.1 MOSFETs

The MOSFET has a resistive behaviour in its on state, and the output characteristic passes through zero. It can conduct a small current with a very low voltage drop.

4.1.1 Zero Current Switch

A MOSFET can be modelled as an ideal switch with a series resistance, and a capacitor connected in parallel - see figure 5. Every time it is turned on, the parallel capacitor is discharged through the resistance and (0.5 x C_{out} x V_{DS}) units are lost. A MOSFET in a Zero Current Switch will have to turn on with a high drain-source voltage, and there will be capacitive switching losses. Additionally, the reactive overcurrent in the switch is very high, and as the MOSFET does not perform well in overcurrent conditions, the conduction losses will be very high. Therefore the MOSFET is not very suitable as a Zero Current Switch.

4.1.2 Zero Voltage Switch

In a Zero Voltage Switch, the MOSFET turns on without any voltage between drain and source, and so there are no capacitive switching losses. There is no reactive overcurrent and the conduction losses are not very important. The MOSFET does have to turn off a current, but as the switching times of a MOSFET are small, the turn off losses will not be excessive.

4.2 IGBTs

The IGBT has a threshold voltage of around 0.7V; a voltage drop lower than this value is not possible. The "resistive part" of the output characteristics of an IGBT is very low, and so it can conduct large currents with a low voltage drop. It is thus most suitable for use at high current densities.

An IGBT can be simply modelled as a pnp-transistor driven by a MOSFET. The disadvantage of this structure is the turn off. If a pnp transistor is to be turned off quickly, a positive base current must be supplied, to force the carriers in the base to recombine and stop the device conducting. In the IGBT, the base of the pnp stage cannot be accessed directly, and so this current cannot be delivered at turn off, meaning that the device continues to conduct while the carriers recombine "naturally". During this time, a current tail appears.

4.2.1 Zero Voltage Switch

In a Zero Voltage Switch, the IGBT must turn off a current. Even if the voltage across the switch rises with a limited dV/dt (sinusoidal waveform), the current tail phenomenon means that turn off losses will be important. Therefore the IGBT is not very suitable for zero voltage switching.

4.2.2 Zero Current Switch

In a Zero Current Switch, the external circuit defines the current in the switch. This current tends to zero, and hence the IGBT does not turn off current, so no tail appears. Another problem that can occur with

:he IGBT, latching, does not occur in this mode. Even if the IGBT latches at the maximum current, it :an turn off later because the current is defined by :he external circuit. The carriers that remained in the ɔase of the pnp-transistor can be recovered by a ɔositive current into the base. In a Zero Current Switch, the negative half wave of the resonant current flows through the antiparallel diode. During that time, a negative voltage is applied to the IGBT. A current flows through the body diode of the internal MOSFET nto the base of the pnp-transistor.

5. TWO-SWITCH RESONANT CONVERTERS

As in standard power converters, for higher power applications, two switches can be connected as shown in figure 6 to form a half-bridge resonant converter. The same passive components are used for the resonance of both switches, and a transformer has been added to drive the load.

5.1 Thyristor Mode

In the example above, the commutation frequency of the switches (f_{sw}) is lower than the resonant frequency of the circuit (f_0). This results in a "dead" zone in the transformer waveform, giving a poor overall efficiency. If the switching frequency is increased, as shown in figure 8, the resonant waveforms overlap and the transformer is used more efficiently. However, the switch now has to turn on at a non-zero current level, and as the diodes turn off at a high current level (e.g. point A in figure 7), losses due to their recovery time will be high.

5.2 Dual Thyristor Mode

The effect of the diode recovery time can be reduced by increasing the switching frequency further - see figure 8. In this case, the diode turns off at zero current.

The main advantage of this type of circuit is that the intrinsic diode of the MOSFET, which has very poor reverse recovery characteristics, can be used in the circuit, removing the need for a further discrete diode.

CONCLUSIONS

Resonant converter topologies can be used to increase circuit switching speeds, allowing the cost of circuit magnetics to be reduced, while still keeping switching losses to a minimum. Full wave rather than half wave topologies are generally used, as they generate less EMI. Capacitive switching losses when turning on with a high drain-source voltage means that MOSFETs are more suitable for Zero -Voltage than Zero-Current switches, while its poor turn-off characteristics mean that the IGBT is more suited to Zero-Current topologies.

Figure 6. Half-Bridge Zero-Current resonant converter

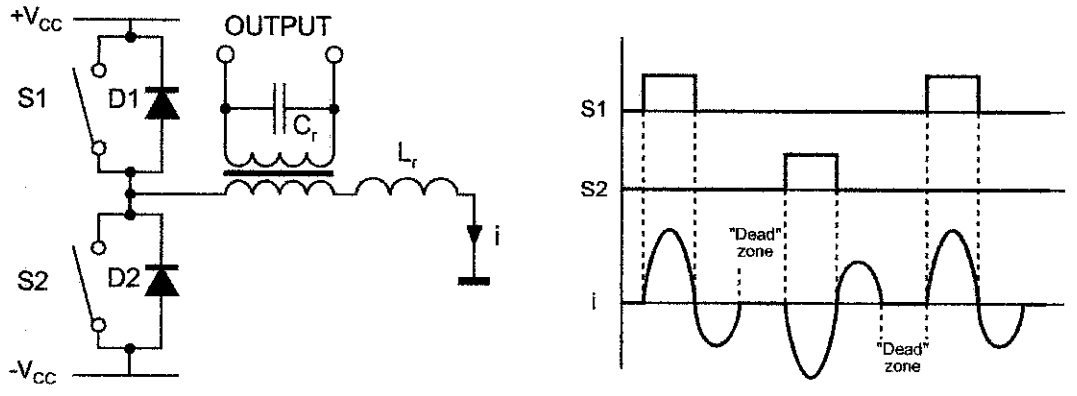

Figure 7. Half-Bridge waveforms with $f_{SW} > f_0$

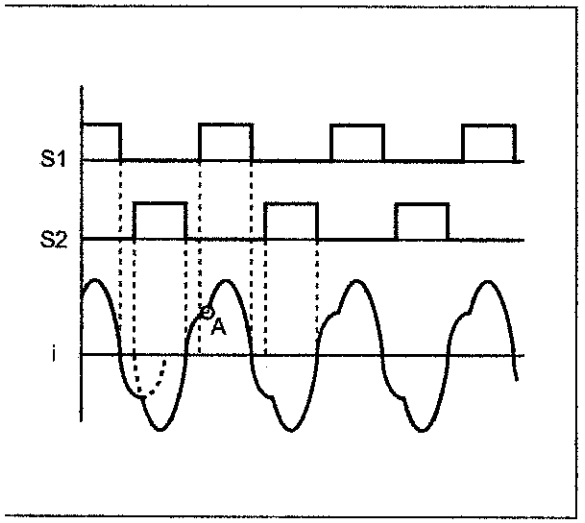

Figure 8. Half-Bridge waveforms with $f_{SW} >> f_0$